COMPUTATION OF RESONANT FREQUENCY OF DUAL BAND TRIANGULAR PATCH ANTENNA

A MASTER'S THESIS

In

Electrical & Electronics Engineering

Atılım University

By

SULTAN CAN

JULY 2011

COMPUTATION OF RESONANT FREQUENCY OF DUAL BAND TRIANGULAR PATCH ANTENNA

A MASTER'S THESIS

In

Electrical & Electronics Engineering

Atılım University

By

SULTAN CAN

JULY 2011

COMPUTATION OF RESONANT FREQUENCY OF DUAL BAND TRIANGULAR PATCH ANTENNA

A THESIS SUBMITTED TO

THE GRADUATE SCHOOL OF NATURAL AND APPLIED SCIENCES

OF

ATILIM UNIVERSITY

BY

SULTAN CAN

IN PARTIAL FULFILLMENT OF THE REQUIREMENTS FOR THE DEGREE OF

MASTER OF SCIENCE

IN

THE DEPARTMENT OF ELECTRICAL ELECTRONICS ENGINEERING

JULY 2011

Approval of the Graduate School of Natural and Applied Sciences, Atılım University.

_____

Prof. Dr. İbrahim Akman

Director

I certify that this thesis satisfies all the requirements as a thesis for the degree of Master of Science.

_____

Assoc. Prof. Dr. Elif Aydın

Head of Department

This is to certify that we have read the thesis "Computation of Resonant Frequency of Dual Band Triangular Patch Antenna" submitted by "Sultan Can" and that in our opinion it is fully adequate, in scope and quality, as a thesis for the degree of Master of Science.

_____

Assoc. Prof. Dr. Elif Aydın

Supervisor

Examining Committee Members

Assoc. Prof. Dr. Ali Kara	_____
Assoc. Prof. Dr. Elif Aydın	_____
Asst. Prof. Dr. Nursel Akçam	_____
.....	_____
.....	_____

Date: 20.07.2011

I declare and guarantee that all data, knowledge, and information in this document has been obtained, processed, and presented in accordance with academic rules and ethical conduct. Based on these rules and conduct, I have fully cited and referenced all material and results that are not original to this work.

Name, Last name: Sultan Can

Signature:

ABSTRACT

COMPUTATION OF RESONANT FREQUENCY OF DUAL BAND TRIANGULAR PATCH ANTENNA

Can, Sultan

M.S., Electrical & Electronics Engineering Department

Supervisor: Assoc. Prof. Dr. Elif Aydın

July 2011, 84 pages

This study focuses on calculating the resonant frequency of equilateral triangular patch antennas and calculation of the operating frequencies of dual-band shorting pin-loaded equilateral triangular patch antennas. Two models are proposed for the purpose of computing of resonant frequency of an equilateral triangular patch antenna of which are based on cavity model analysis and use effective side-length expression. The first model utilizes dynamic permittivity and the second one uses effective permittivity expressions, respectively. The results obtained from these models are compared with the theoretical, simulated (CST), and experimental results. The conformity in between the results obtained in this paper is closer when compared to the literature. This study also presents the computation of resonant frequencies of the dual frequency, shorting pin-loaded, equilateral triangular microstrip patch antennas. A Shorting pin is loaded to an equilateral triangular patch antenna in order to form a dual frequency operation. An empirical formula is developed for the calculation of upper and lower frequencies of a shorting pin-loaded equilateral triangular patch. The results are compared with the measured values as well as those obtained from the transmission line model. The results of both equilateral triangular patch and the shorting pin-loaded dual frequency triangular patch models are presented and discussed.

Keywords: Equilateral triangular patch antenna, resonant frequency, dual-frequency patch antenna, operating frequency, shorting-pin.

ÖZ

ÇİFT FREKANSLI ÜÇGEN YAMA ANTENLERDE REZONANT FREKANSININ HESAPLANMASI

Can, Sultan

Yüksek Lisans., Elektrik & Elektronik Mühendisliği Bölümü

Tez Yöneticisi: Doç. Dr. Elif Aydın

Temmuz 2011, 84 sayfa

Bu çalışmada, eşkenar üçgen yama antenlerin ve çift frekanslı eşkenar üçgen yama antenlerinin çalışma frekanslarının hesaplanması üzerinde durulmuştur. Eşkenar üçgen yama antenin rezonant frekanslarının bulunmasında iki model önerilmiştir. Önerilen her iki model kovuk modeli ile analiz edilmiş olup etkin kenar uzunluğu ifadeleri kullanılmıştır. Birinci ve ikinci modellerde sırası ile dinamik ve etkin dielektrik sabiti ifadelerine yer verilmiştir. Modellerin sonuçları CST benzetimi sonuçları, deney sonuçları ve literatürdeki teorik sonuçlar ile kıyaslanmış, daha kesin sonuçlar elde edilmiştir. Çalışmada çift frekanslı eşkenar üçgen yama antenlerin çalışma frekanslarının hesaplanmasına da yer verilmiştir. Çalışmadaki anten kısa devre iğnesi ile kısa devre yapılarak, çift frekanslı eşkenar üçgen oluşturulmuştur. Üst ve alt frekanslarının hesaplanmasında empirik bir formül geliştirilmiştir. Sonuçlar ölçüm sonuçları ve iletim hattı modeli sonuçları ile kıyaslanmıştır. Tüm sonuçlar literatür değerleri ile kıyaslanıp, tartışılmıştır.

Anahtar kelimeler: Eşkenar üçgen yama antenleri, rezonans frekansı, çift-frekanslı yama antenler, çalışma frekansları

To My Family

Who dedicate their lives to my happiness, education, and development.

ACKNOWLEDGEMENT

I owe my deepest gratitude to my dear advisor Assoc. Prof. Dr. Elif Aydın for her patience, motivation, and immense knowledge. Her guidance helped me in every single moment in research and writing of this thesis. This thesis would not have been possible unless her guide and support. She was not only a scientific advisor but also she brightens my life.

I would like to thank the rest of my thesis committee: Assoc. Prof. Dr. Ali Kara and Asst. Prof. Dr. Nursel Akçam for their participation.

I also would like to thank Prof. Dr. Özlem Aydın Çivi for letting me to use HFSS in the concept of European School of Antenna.

The last but not the least; I would like to thank my family members, my mother Şenay Can, my father Yakup Can, my sister G. Nurdan Can and to S. Sevcan Kolçak. I will always remember their sacrifice, love, care, support, and encouragement.

TABLE OF CONTENTS

LIST OF TABLES

LIST OF FIGURES

LIST OF ABBREVIATIONS

PCF	- Permittivity Correction Factor
SATCOMS	- Satellite Communications
TEM	- Transverse Electromagnetics
GPS	-Global Positioning Systems
ETMP	-Equilateral Triangular Microstrip Patch
ETMA	-Equilateral Triangular Microstrip Antenna
MA	-Microstrip Antenna
CST	-Computer Simulation Technology
TLM	-Transmission Line Model
FR	-Frequency Ratio
APE	-Average Percentage Error
HFSS	-High Frequency Structure Simulator

CHAPTER 1

INTRODUCTION

Antennas are one of the most important and critical elements in today's communication systems. A well-designed antenna can increase the overall performance of the system. Antennas are the system elements designed for receiving or transmitting electromagnetic waves. In other words, an antenna is a kind of electromagnetic converter. As a transmitter, antennas give the electromagnetic waves into a transmission line and as a receiver; they act as an element, which recognize the electromagnetic waves.

Microstrip patch antennas, which play a significant role in wireless communications, are becoming increasingly popular due to their advantages. The term "microstrip" was first proposed by Deschamps [1] in 1953 and was demonstrated in 1970's by Munson [2]-[3] and was developed by Howell [4]. In the recent years, especially with the wide spread use of mobile phones, wireless communication devices and GPS have made the microstrip antennas more preferable.

A microstrip antenna consists of a ground on one side and a radiating patch on the other side of the dielectric substrate. This radiating patch is made of conducting materials such as gold and copper. The conducting patch can be designed in any desired shape. As microstrip technology requires, the radiating patch and the feed lines are photo etched on the dielectric substrate. The radiation causes the fringe field effects and because of fringing fields between the patch edge and the ground plane, the microstrip patch radiates primarily. A thick dielectric substrate with low dielectric constant desired to provide larger bandwidth, better efficiency, and better radiation. However, all these parameters lead to a larger physical size of an antenna.

Microstrip patch antennas are widely used due to their advantages. Microstrip patch antennas have thin profile, lightweight, low cost, low volume. Moreover, they can be integrated with circuits and can be made conformal. Furthermore, simple arrays can be easily created. They also support both linear and circular polarization according to the feed and they are capable of dual and triple frequency operations.

However, they have low efficiency, small bandwidth, and temperature tolerance problems. They require high quality substrate and good temperature tolerance. High-performance arrays require complex feed systems and polarization purity is difficult to achieve. Low gain, low power handling capacity, and surface wave excitation are other disadvantages of the microstrip patch antennas.

There are various applications of microstrip patch antennas. They are used in aircrafts (communication and navigation altimeters) and in missiles and telemetry (stick-on sensors, proximity fuzes, millimeter devices). In addition, they are used in missile guidance (seeker monopulse arrays, integral radome arrays) and in adaptive arrays (multi-target acquisition, semiconductor-integrated array). Moreover they are preferred in battlefield communications and surveillance (flush mounted on vehicles) and in SATCOMS (vehicle-based antenna, switched-beam array), in mobile radio (pagers and hand telephones, man pack systems), in reflector feeds (beam switching), in remote sensing (large lightweight apertures), in biomedical applications (microwave cancer therapy) and in convert antennas (industrial alarms, personal communications).

Common use of microstrip patch antennas in our daily lives has made them more popular. Demand on reducing the size of the microstrip patch antennas has increased the interest in them. According to type of the application, the shape of the patch varies. The common basic shapes are rectangular, triangular, circular, annual ring etc.

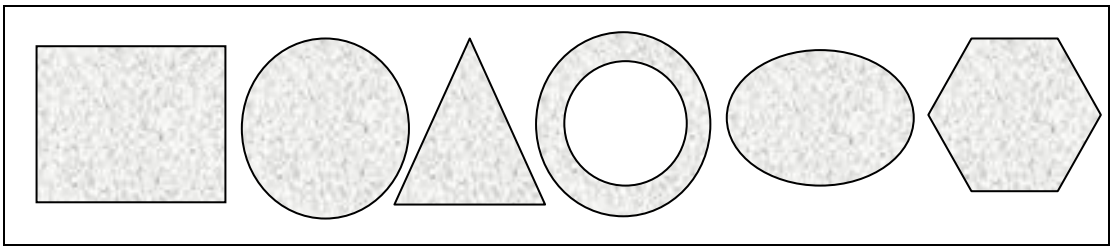

Figure 1: Basic shapes of microstrip patch antennas

Triangular microstrip patch antennas are one of the widely used patches in wireless communications. Among those, the equilateral triangular patch antenna is one of the most important and common ones. Even though these patches have advantages with their small size and low cost, they have disadvantage with their narrowband property. Due to their outstanding and positive features, they are popular both in industrial applications and in research-based studies.

Because of the narrow bandwidth of the equilateral triangular microstrip antenna, with and without air-gap, accurate computation of the resonant frequency is a crucial task for the efficient design of such antennas. Accordingly, these studies take considerable interest in the literature by various authors. Mainly, they propose the usage of various methods and approximations on the computation of resonant frequency [5] - [15] .

In the literature, there are several analyzing models for defining the parameters of microstrip patches. Among those, the method of moments and the cavity models are the most used models. Although the moment method is the more accurate, because of its complexity and time-consuming computational structure, the cavity model is the more preferred one. In the cavity analysis, a microstrip antenna is modeled with a resonant cavity having electric and magnetic walls. Here the effective dimensions of the antenna and the effective dielectric constant of the substrate expressions are required to correct perfect magnetic wall assumption and account for the fringing fields and the dispersion effect [7].

Since the resonant frequency depends on the patch structure, the only way to change the resonant frequency of an equilateral microstrip patch is to manufacture the

structure. A tunable resonant characteristic with a two-layer structure is achieved by adjusting an air-gap layer among the substrate and the ground.

Multi-frequency applications are needed in various communication systems. Demand on the multi-band operations of the communication systems caused an interest on dual-band operations, and various studies have been done to accomplish dual-frequency operation in [32]-[48]. Stacked rectangular and equilateral triangular microstrip antenna (ETMA) have been demonstrated for dual band application in [34], dual-frequency designs have been described [32]-[48], slot-loaded ETMA have been investigated in [33], [38], [39], [40] and shorting pin-loaded equilateral triangular microstrip patches have been presented in [42]-[48].

Due to their low cross section, microstrip patch antennas are widely used in many wireless systems like satellite positioning systems where the system commonly requires a multi-band operation commonly. The microstrip patches have low profile and lightweight but even these antennas sizes are too large to fit in a low frequency communication system.

The studies in literature proved that loading a shorting pin significantly reduced the size of antenna at a given operating frequency [44].It is also mentioned that there is a ratio between two operating frequencies (about 1.3-2) [42]. In some applications, greater frequency ratio is needed. Since the ratio between two frequencies is limited with inserting a shorting pin, by inserting a circuitry, the designers try to increase the ratio for various applications [44]-[45]. SAR (synthetic aperture radar) is one of these applications, which require larger frequency ratio.

The feed position is within one or several millimeter distances from the shorting pin position, which may cause manufacturing problem. However, the designer achieves higher frequency ratios by inserting a shorting pin to an equilateral triangular patch. Size reduction is another advantage of a shorting pin-loaded microstrip antenna for the same operating frequencies. This higher ratio corresponds to larger upper frequency and smaller lower frequency for different pin positions and different permittivity values of the substrate. As mentioned in literature, the frequency ratio of a triangular patch with shorting pin is larger than the shorting pin-loaded rectangular

and circular patches [41]. It is also underlined that the size of a triangular patch reduces after inserting a shorting pin as one third of the antenna at the same operating frequency [44]. There are several studies, which presented the characteristics of triangular patch with shorting pin [42]-[48].

In this study, the resonant frequency of an equilateral triangular microstrip antenna is accurately determined via cavity analysis using a simple effective permittivity and patch radius expressions including modal effects. The air-gap tuning effect on the resonant frequencies of equilateral triangular microstrip antenna is also presented in this study. As a result, with the proposed procedure, accurate resonant frequency values is obtained exhibiting small percentage error values with respect to the previous models. A dual-band equilateral triangular patch antennas upper and lower operating frequencies are calculated in this study, as well. A shorting-pin is inserted to obtain dual-frequency operation. Cavity model is used to analyze the upper and lower operating frequencies. The upper and lower resonant frequencies of a shorting pin-loaded equilateral triangular patch antenna depend on the structure of the antenna and it is not possible to change the operating frequencies without producing a new structure. The effects of shorting-pin position and the permittivity effects are also investigated in this study.

In Chapter 2, the substrate technologies of microstrip patch antennas are demonstrated. Feed techniques of the patch antennas are also presented. Microstrip line feed, aperture-coupled feed technique, proximity coupled feed, coaxial feed techniques are also presented, and methods for analyzing the patch are indicated. Transmission line models and cavity models are demonstrated respectively.

In Chapter 3, literature review for calculating the resonant frequency of an equilateral triangular patch antenna and literature review for dual-frequency equilateral triangular patch antenna are demonstrated. The results obtained from the literature are shown for both resonant frequency of an equilateral triangular patch antenna and the resonant frequencies of a shorting pin-loaded equilateral triangular patch antenna.

In Chapter 4, calculation of resonant frequency of an equilateral triangular patch antenna is presented with two proposed methods, which use dynamic and effective

permittivity values, respectively. Both models' comparison is done with the studies in literature and CST simulation results.

In Chapter 5, shorting pin-loaded dual-frequency equilateral triangular patch antennas are presented. Upper and lower frequencies of these antennas are calculated and compared with the results presented in other studies. A study of two shorting pin-loaded triangular patch antenna is also demonstrated as a future study.

In Chapter 6, the results obtained from the whole study are summarized. Comparison and errors are also concluded with respect to the results, which are obtained from the literature. Future work is presented.

CHAPTER 2

MICROSTRIP TECHNOLOGY; FEED AND ANALYSIS TECHNIQUES

2.1 Substrate technology

Substrate technology is a key element in printed antenna technology, so in microstrip antenna as well. Microstrip antennas are made of plastic substrates and alumina in early stages of printed technology but nowadays, lower permittivity substrates are getting increasingly popular. The use of lower permittivity reduces the surface-wave effects but feeder radiation is then more difficult to suppress [21]. Printed elements generally use synthetic elements instead of ceramics although ceramics are best to use in printed antennas. Ceramics are expensive and mass production and it is hard to give shape for a ceramic substrate.

Table 1: Some substrate examples and their permittivity values, which are used in microstrip technology.

ε_r	**Material**
1.0	Aeroweb (honeycomb)
1.06	Eccofoam PP-4
2.10	RT Duroid 5880 (microfiber Teflon glass laminate)
2.32	Polyguide 165 (polyolefin)
2.52	Fluorglas 600/1 (PTFE impregnated glass cloth)
3.20	Schaefer dielectric material, PT (polystyrene with titania filler)
3.75	Kapton film (copper clad)
10.2	RT Duroid 6010
11	Sapphire

2.2 Feed Techniques

There are various methods of feeding in microstrip patch antennas. The methods are categorized into two as contacting and non-contacting methods. The Difference between contacting and non-contacting methods is stated as; in contacting method, RF power directly feeds the patch by contacting the patch like a microstrip line. In non-contacting method electromagnetic field coupling is applied for transferring power between the microstrip line and the radiating patch. The microstrip line, coaxial probe, aperture coupling, and proximity coupling are some of the most used feed techniques [20].

2.2.1 Microstrip Line Feed

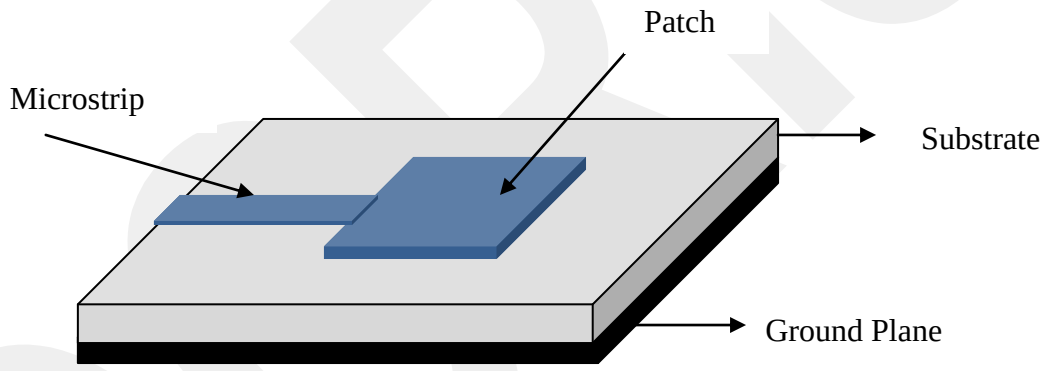

Figure 2 : Microstrip line feed geometry

A conducting strip, which is smaller in width compared to the patch dimension, is directly connected to the microstrip patch as shown in Figure.2. Feed can be etched on the same substrate with this process. This process is an advantage to provide planar structure. Impedance of the feed line is matched with no additional matching element since there is an inset cut in the patch. Controlling the inset cut position helps the designers to achieve matching the patch and feed line. Simplicity and ease of fabrication are also provided with this process. “However as the thickness of the dielectric substrate increases, surface waves and spurious feed radiation also

increases, which hampers the bandwidth of the antenna [17] .” “The feed radiation also leads to undesired cross-polarized radiation [20].”

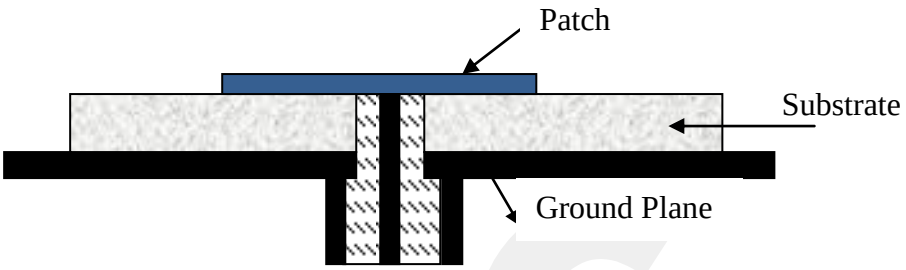

Figure 3: Coaxial feed geometry

The Coaxial feed or probe feed is a very common technique used for feeding microstrip patch antennas, which will be mentioned in details in 2.2.4.

2.2.2 Aperture-Coupled Feed Technique

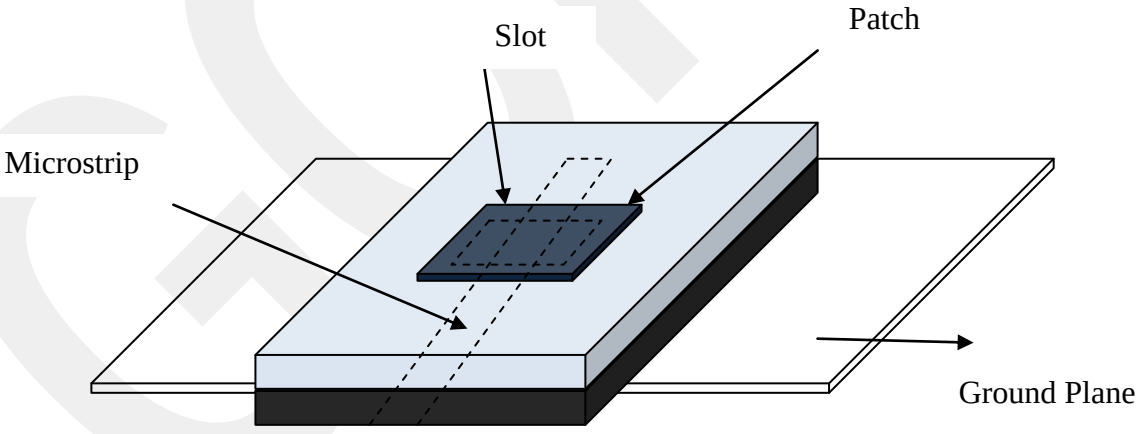

Figure 4: Aperture-coupled feed geometry

In aperture-coupled feed technique, a ground plane separates the microstrip feed line and the radiating patch as shown in Figure.4. An aperture or a slot in the ground plane makes coupling between the feed line and the patch. Due to the symmetry of

the configuration, lower cross polarization occurs because of the coupling aperture position, which is centered under the patch. Shape, size, and location parameters are taken into account to determine the amount of the coupling from the feed line to the patch. The ground plane that separates the ground and feed line minimizes spurious radiation. For the optimization of radiation from the patch, a high dielectric material is preferable for the substrate below the ground plane. A thick, low dielectric constant material is used for the substrate above the ground plane [17]. As a drawback, this feeding scheme provides narrow bandwidth; it has manufacturing problems for multi-layer designs that also increases the antenna size.

2.2.3 Proximity-coupled Feed

Proximity coupled feed which is also called electromagnetic coupling feed is shown in Figure. 5.Microstrip line feed is located in between two different substrates as drawn. The radiating patch settled on the top of the substrate.

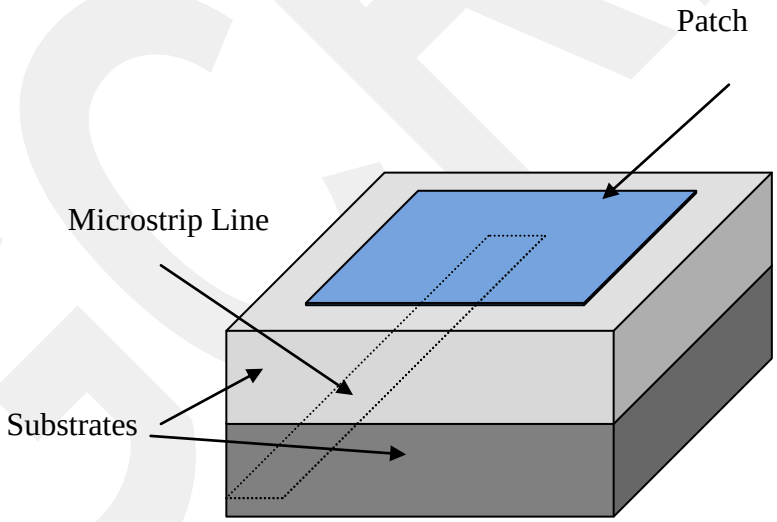

Figure 5 : Proximity-coupled feed geometry

As a drawback, the thickness of the antenna increases if the thickness of the two-layer substrates increases. As the thickness increases, the size of the antenna also increases. However, this geometry provides very high bandwidth. The spurious feed

radiation is eliminated with this technique [17]. Matching depend on the width to line ratio and the length of the microstrip line feed and can be controlled by these parameters as well. Proper alignment is needed in this configuration, which causes fabrication difficulties in double layer antenna.

The comparisons of feed techniques are stated in [16], and listed in table 2.

Table 2: Comparison of the presented feed techniques.

Characteristics	**Microstrip line feed**	**Coaxial feed**	**Aperture coupled feed**	**Proximity coupled feed**
Spurious feed radiation	More	More	Less	Minimum
Reliability	Better	Poor due to soldering	Good	Good
Ease of fabrication	Easy	Soldering and drilling needed	Alignment required	Alignment required
Impedance matching	Easy	Easy	Easy	Easy
Bandwidth (achieved with impedance matching)	2-5 %	2-5 %	2-5 %	13%

2.2.4 Coaxial Feed technique

Coaxial fed is used in this thesis to feed an equilateral triangular antenna as illustrated in Figure 6. The inner conductor of the coaxial probe is soldered to the patch and outer part is connected to the ground. Fabrication of the coax-feed is easy and it has low spurious radiation. Moreover, input impedance matching can be changed with the change of the feed position and these features are the advantages of the coax-feed.[20]

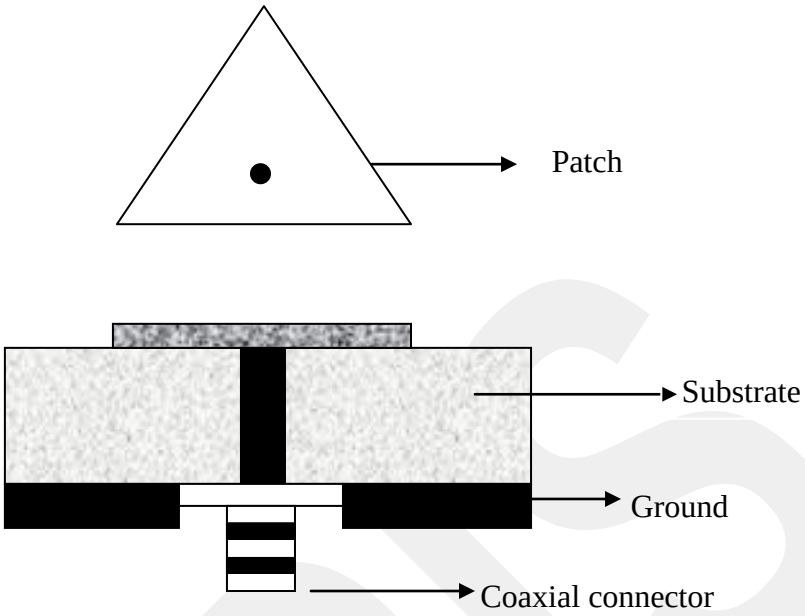

Figure 6: Geometry of a coax-feed patch

However, narrow bandwidth and difficulty of the modeling are the drawbacks. The feed is inserted to the hole, which is drilled in the substrate. The feed thickness is larger than the total thickness of the substrate and the ground plane. Therefore, a bulge occurs outside the ground plane. Because of this procedure for thick substrates ($h>0.02\lambda_0$) it does not become planar. The larger thicknesses cause matching problems. Input impedance become more inductive since the probe length increases for thicker substrates. It is concluded that, thick dielectric substrate patches suffer from impedance matching although it provides broad bandwidth [20].

2.3 Method of analysis

Basic geometry of a microstrip antenna with a coaxial feed is drawn in Figure 7. As seen in side view of the patch the z-axis is perpendicular to the conducting patch. The electromagnetic waves are first guided along the coaxial and after this; it spread out under the patch. Electromagnetic waves reach the boundary of the patch after spreading out under the patch so some of the electromagnetic waves are reflected and some of them radiated into the space.

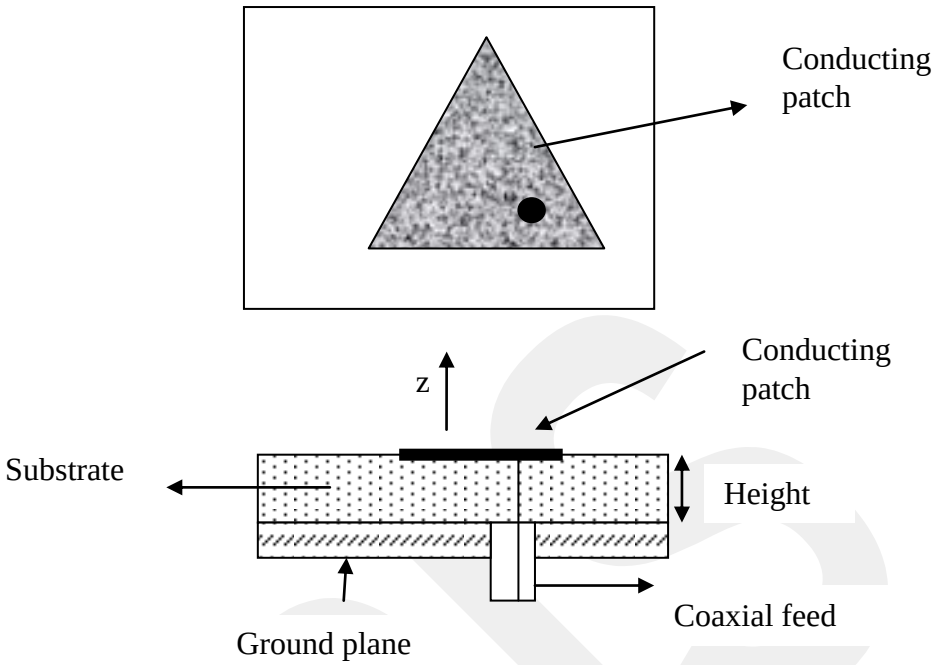

Figure 7: Geometry of a triangular patch fed by a coax probe.

There are two lines of approach to distinguish the radiation fields;

i. Finding current distributions along the antenna structure and obtain the radiation fields from these current sources.
ii. Finding the fields at the exit region and since these field acts as an equivalent source, the radiation fields are obtained by these fields [21].

Based on these approaches mentioned in i and ii, several methods are developed to analyze microstrip patches. Transmission line model, full wave model and cavity model are the most popular methods of analysis for microstrip antennas [17].

2.3.1. Transmission Line Model

This model represents the microstrip antenna with two slots of width *W* and height *h* separated by a transmission line of length L [20]. The microstrip is essentially an inhomogeneous line of two dielectrics, typically the substrate and air as seen in figure 8.

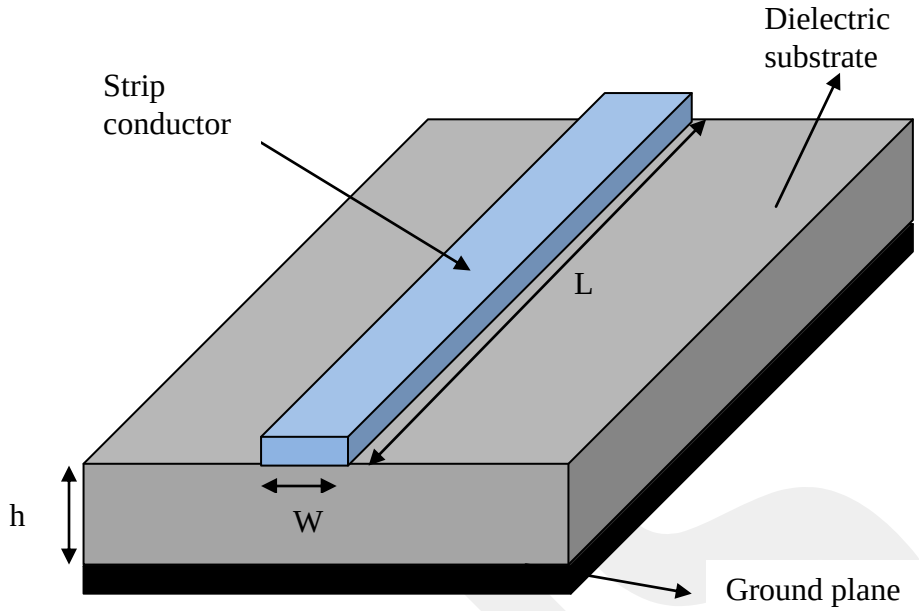

Figure 8: Microstrip line geometry

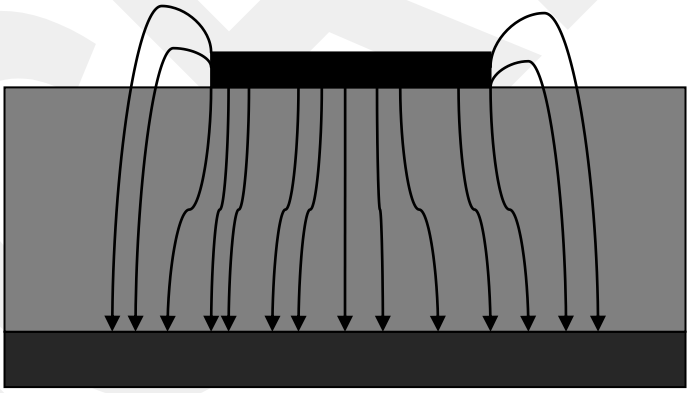

Figure 9: Electric field lines distribution

Some parts of the electric field lines are settled in the air although the most of the electric field lines are located in the substrate. The phase velocities are different in various materials. In this situation, it is different in air and in the substrate. As a result, this transmission line cannot support pure transverse electric-magnetic (TEM) mode of transmission [20]. Fringing field effects occur because of this process so an effective dielectric constant should be calculated in order to count wave propagation of line and fringe field effects. It is concluded that the effective dielectric constant is hardly less than the dielectric constant since electric field around periphery of the

patch is not confined in the substrate as seen in Figure.9 [20]. The expression for ε_{reff} is given by Balanis [17] as:

$$\varepsilon_{reff} = \frac{\varepsilon_r + 1}{2} + \frac{\varepsilon_r - 1}{2}\left[1 + 12\frac{h}{W}\right]^{-\frac{1}{2}} \quad (1)$$

ε_{reff} =effective dielectric constant

ε_r =dielectric constant of substrate

h=height of dielectric substrate

W= width of the patch

2.3.2. Cavity model

The transmission line model is the simplest method between these two analyses and gives a good physical insight but this model is less accurate. In its original form the transmission line model is limited to rectangular and circular patches, however extension to other patches is also possible. The full wave models are very accurate but give less physical insight compared to the other methods. It requires considerable computational time and effort but provide little physical insight. Moreover, the cavity model is more accurate and gives good physical insight but complex in nature. Cavity model has less computational time and effort compared to other methods. Although the other methods are easy to use, except the consuming time, they have some drawbacks, that they ignore the field variations along the radiating edges. These drawbacks can be overcome by cavity model.

Microstrip antennas can be assumed, as they are dielectric-loaded cavities. The region between the patch and the ground plane is the normalized fields within the dielectric substrate. This normalized field can be found more accurately by treating that the region is a cavity bounded by the electric conductors (above and below it) and magnetic walls (to simulate and open circuit) along the perimeter of the patch [17]. Cavity model is an approximate model that fundamentally does not radiate any power and leads to a reactive input impedance of zero or infinite value of resonance. “However, assuming that the actual fields are approximate to those generated by

such a model, the computed pattern, input admittance and resonant frequencies compared with the measurements." [17]

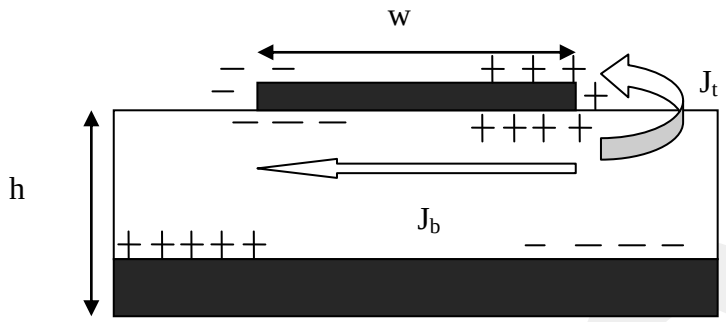

Figure 10: Geometry of current division in cavity model.

As shown in the Figure 10, charge distributions, seen on the top and the bottom of the patch. This distribution occurs when the microstrip patch is energized. Charge distribution is established on the upper and lower surfaces of the patch. Charge distribution on the ground is also seen after the patch is powered. The distribution is controlled by two mechanisms; one is attractive mechanism and the other is repulsive mechanism as discussed in [19]. The attractive mechanism occur in between the opposite charge lie on ground plane and the charges on the top of the patch. This configuration helps to keep the charge concentration intact at the bottom. The repulsive mechanism occurs in between same charges stated in the bottom of the patch. These charges push some charges from the bottom to the top of the patch. Charge movements cause current flow at the top and the bottom surface of the patch.

The ratio of height of the substrate to width of the patch is very small in cavity method with an assumption. The attractive mechanism dominates and causes most of the charge concentration and the current below the patch surface while the height to width ratio further decreases. Much less current would flow on the top surface of the patch. "The current on the top surface of the patch would be almost equal to zero, which would not allow the creation of any tangential magnetic field components to the patch edges. [19] Hence, the four sidewalls could be modeled as perfectly magnetic conducting surfaces. This implies that the magnetic fields and the electric field distribution beneath the patch would not be disturbed.

However, in practice, a finite width to height ratio would be there and this would not make the tangential magnetic fields to be completely zero. But they are being very small; the side walls could be approximated to be perfectly magnetic conducting" [16]. It should be also considered that treating a microstrip antenna only as a cavity would not be a sufficient way to find the absolute values for electric and magnetic fields. In fact, the cavity would not radiate and its input impedance would be purely reactive by treating the walls of cavity as well as the material in it as lossless.

Effective loss tangent is expressed as in [19]:

$$\delta_{eff} = \frac{1}{Q_T} \tag{2}$$

Q_T is the total quality factor and defined as :

$$\frac{1}{Q_T} = \frac{1}{Q_d} + \frac{1}{Q_c} + \frac{1}{Q_r} \tag{3}$$

Q_d is the quality factor of the dielectric and given as eqn.4 where ω_r is the angular frequency, W_T is the total energy stored in the patch at resonance, P_d is the dielectric loss and $tan\delta$ is the loss tangent of the dielectric :

$$Q_d = \frac{\omega_r W_T}{P_d} = \frac{1}{tan\delta} \tag{4}$$

Q_c is the quality factor of the conductor and expressed as eqn.5 where P_c is the conductor loss, Δ is the skin depth of the conductor and h is the height of the substrate :

$$Q_c = \frac{\omega_r W_T}{P_c} = \frac{h}{\Delta} \tag{5}$$

Q_r is the quality factor for radiation and given as eqn.6 where ω_r is the angular frequency, W_T is the total energy stored in the patch at resonance and P_r is the power radiated from the patch:

$$Q_r = \frac{\omega_r W_T}{P_r} \tag{6}$$

These equations yield the total effective loss tangent of the microstrip patch antenna defined as:

$$\delta_{eff} = tan\delta + \frac{\Delta}{h} + \frac{P_r}{\omega_r W_T} \tag{7}$$

CHAPTER 3

LITERATURE REVIEW

3.1 Literature review for calculating the resonant frequency of an equilateral triangular patch

There are various studies in the literature, which use different expressions and models to analyze the resonant frequency of the equilateral triangular patch antennas. In this chapter, several studies will be presented before the expression studied in this thesis. Ç. S. Gürel and E. Yazgan presented one of the studies for finding the resonant frequency in [6].

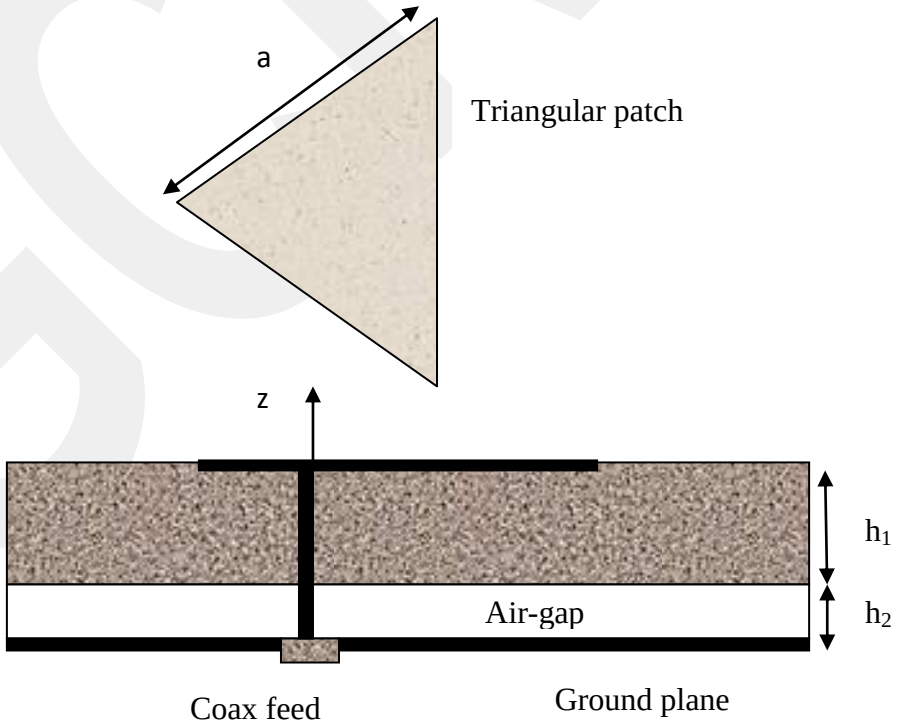

Figure 11: The geometry of the tunable equilateral triangular patch [6].

A new dynamic permittivity expression is formulated and resonant frequency of equilateral triangular patch is determined by the new dynamic permittivity expression. The proper side-length expression is given and it is obtained that this model achieved more accuracy if it is compared to the moment method and the studies done before this study. The detailed results are also given in this study.

This study is done for both low and high substrate permittivity cases. The structure also generalized for two-layer structure in order to determine air-gap tuning effect. The geometry of the tunable equilateral triangular patch is given in figure 11;

The cavity model, depending on the perfect magnetic wall assumption, is used to analyze the resonant frequency. The resonant frequency formulation is given as:

$$f_{mnl} = \frac{2}{3(\varepsilon_{r2})^{1/2}}(m^2 + mn + n^2)^{1/2} \tag{8}$$

where c is the speed of light in free space, a is patch side lengt, ε_{r2} is relative permittivity of the substrate m, n, l are integers that cannot be zero simultaneously and the eqn. 9 should be considered:

$$m + n + l = 0 \tag{9}$$

The h is defined as the total thickness of the substrate as:

$$h = h_1 + h_2 \tag{10}$$

h_1 is the thickness of the air-gap and h_2 defined as the thickness of the substrate height. The formulation can be converted into single-layer by reducing the air-gap thickness to the zero. Since the air-gap thickness is zero the patch has single-layer structure.

Equivalent relative permittivity of the substrate is formulated as in eqn.11, which is related with the thicknesses of the substrates and the substrate relative permittivity:

$$\varepsilon_{req} = \frac{\varepsilon_{r2}(h_1 + h_2)}{(h_2 + \varepsilon_{r2} h_1)} \tag{11}$$

The dynamic dielectric permittivity is defined as:

$$\varepsilon_{dyn} = \frac{C_{dyn}(\varepsilon_{r0}, \varepsilon_{req})}{C_{dyn}(\varepsilon_{r0} = \varepsilon_{req} = 1)} \tag{12}$$

where

$$C_{dyn}(\varepsilon_{req}, \varepsilon_{r0}) = C_{0,dyn}(\varepsilon_{req}, \varepsilon_{r0}) + C_{e,dyn}(\varepsilon_{req}, \varepsilon_{r0}) \tag{13}$$

$C_{e,dyn}$ is the total dynamic fringe capacitance and $C_{0,dyn}$ is the main field capacitance.

In order to obtain the total dynamic fringe field capacitance $C_{e,dyn}$, the equilateral triangular patch is replaced with a circular patch having an equivalent surface area. The radius of this circular patch is obtained as:

$$r = \left(\frac{a^2 3^{0.5}}{4\pi}\right)^{1/2} \tag{14}$$

The total dynamic fringe capacitance $C_{e,dyn}$ of the original structure is taken in the form given in [24] as:

$$C_{e,dyn} = \frac{\varepsilon_0 \varepsilon_{req} A}{2h} C \tag{15}$$

A is the physical area of the triangle and the function C is given as :

$$C = \left\{1 + \frac{2h}{\pi\varepsilon_{req}\, r}\left[\ln\left(\frac{r}{2h}\right) + \left(1.41\varepsilon_{req} + 1.77\right) + \frac{h}{r}(0.286\varepsilon_{req} + 1.65)\right]\right\}^{1/2} \tag{16}$$

The total dynamic main-field capacitance $C_{0,dyn}$ expression for an equilateral triangular microstrip patch is taken in a similar form to that of the rectangular microstrip patch having the equivalent surface area [25] as:

$$C_{0,dyn} = \frac{C_{o,stat}}{\gamma_n \gamma_m} \tag{17}$$

$C_{0,stat}$ is given as in eqn. 18 is the static main capacitance:

$$C_{0,dyn} = a^2 3^{0.5} \varepsilon_0 \varepsilon_{req} / 4h \tag{18}$$

and

$$\gamma_{i(i=n,m)} = \begin{cases} 1, i = 0 \\ 2, i \neq 0 \end{cases} \tag{19}$$

In order to include the fringe field effects, the patch side-length r must be replaced with the effective side-length r_e and effective area is formulated as a_e as:

$$a_e = 2r_e \pi^{0.5} / 3^{0.25} \tag{20}$$

In this analysis, r_e is modified for a two-layer structure by assuming that the field is concentrated inside the upper dielectric layer and taken as:

$$r_e = r\left\{1 + \frac{2h}{\pi\varepsilon_{r2} r}\left[\ln\left(\frac{r}{2h}\right) + (1.41\varepsilon_{r2} + 1.77) + \frac{h}{r}(0.268\varepsilon_{r2} + 1.65)\right]\right\}^{\frac{1}{2}} \tag{21}$$

Another expression for an effective patch side-length expression of the single-layer structure was given in a simpler form in [22] as:

$$a_e = a + h(1.2 + \frac{2.25}{\sqrt{\varepsilon_{eff}}}) \tag{22}$$

where ε_{eff} was defined as the effective substrate permittivity and is taken in this study as :

$$\varepsilon_{eff} = \frac{1}{2}(\varepsilon_{r2} + 1) + \frac{1}{2}(\varepsilon_{r2} - 1)(1 + \frac{12h}{3^{0.25}\, a/2})^{-\frac{1}{2}} \tag{23}$$

It is mentioned that the resonant frequency of an equilateral triangular microstrip patch is determined from the cavity model by using a new dynamic permittivity expression combined with the proper side-length extension formula. The formulation is examined for various studies and the errors stated in the following tables;

Table 3: Comparison of measured and normalized theoretical resonant frequencies, a=10cm, ε_{r2}=2.32, h_1 =0, h_2=1.59mm.

Mode	**[13]**	**[11]**	**[12]**	**[23]**	**[13]**	**[13]**	**[8]**	**[9]**	**[21]**	**[6]**
TM_{10}	1280	1.015	0.995	1.047	1.006	1.013	1.000	1.007	1.001	0.998
TM_{11}	2242	1.004	0.983	1.035	1.008	1.001	0.989	0.996	0.990	0.992
TM_{20}	2550	1.019	0.998	1.051	1.024	1.016	1.004	1.011	1.005	1.002
TM_{21}	3400	1.011	0.0991	1.042	1.016	1.008	0.996	1.003	0.997	0.999
TM_{30}	3824	1.020	0.999	1.051	1.013	1.016	1.004	1.012	1.005	1.003
APE (%)		1.39	0.67	4.51	1.33	1.08	0.46	0.74	0.48	0.30

As shown in Table.3 satisfactory agreement is obtained when compared to the literature in the study with an average error of 0.3%. The average error remained in between 0.46 -4.51 % in the previous studies for the proposed antenna.

Table 4: Comparison of measured and normalized theoretical resonant frequencies, a=8.7cm, ε_{r2}=10.5, h_1 =0, h_2=0.7mm.

Mode	**[13]**	**[11]**	**[12]**	**[23]**	**[13]**	**[13]**	**[8]**	**[9]**	**[21]**	**[6]**
TM_{10}	1489	1.007	0.994	1.029	1.006	1.006	0.998	1.003	1.000	0.997
TM_{11}	2596	1.001	0.998	1.022	1.005	0.999	0.991	0.996	0.993	0.994
TM_{20}	2969	1.011	0.997	1.032	1.007	1.009	1.001	1.005	1.003	1.000
TM_{21}	3968	1.001	0.987	1.022	1.002	0.999	0.997	0.995	0.993	0.993
TM_{30}	4443	1.013	0.999	1.035	1.008	1.011	1.003	1.008	1.006	1.003
APE (%)		0.66	0.67	2.80	0.57	0.57	0.48	0.50	0.44	0.37

Two other antennas proposed in tables 4 and 5, which have different side-length, permittivity, and thickness values. The proposed method in the afore-mentioned paper achieved good conformity with an average error of 0.37 % and 0.76%.

Table 5: Comparison of measured and normalized theoretical resonant frequencies, a=4.1cm, ε_{r2}=10.5, h_1 =0, h_2=0.7mm.

Mode	**[13]**	**[11]**	**[12]**	**[23]**	**[13]**	**[13]**	**[8]**	**[9]**	**[21]**	**[6]**
TM_{10}	1519	0.986	0.984	1.038	1.002	0.993	0.995	0.981	0.988	0.986
TM_{11}	2637	0.984	0.981	1.036	1.006	0.991	0.992	0.979	0.986	0.984
TM_{20}	2995	1.001	0.998	1.053	1.010	1.008	1.009	0.995	1.003	1.000
TM_{21}	3973	0.998	0.995	1.050	1.016	1.005	1.006	0.992	0.999	0.997
TM_{30}	4439	1.012	1.010	1.066	1.018	1.020	1.021	1.007	1.015	1.012
APE (%)		0.90	1.04	4.85	1.05	0.96	0.97	1.20	0.86	0.76

Table 6: Comparison of measured and normalized theoretical resonant frequencies for high substrate permittivity value and several substrate thickness TM_{10} mode, a=10cm, ε_{r2}=10, h_1 =0.

h_2 (mm)	[13]	[11]	[12]	[23]	[8]	[21]	[6]
4	639	0.977	0.975	1.062	0.989	0.973	0.980
8	631	0.978	0.977	1.098	0.983	0.951	0.970
12	619	0.985	0.989	1.129	0.977	0.928	0.964
16	608	0.991	1.000	1.152	0.966	0.903	0.957

The effects of the permittivity and thicknesses are stated in the tables 6 and 7. Two-layer geometry is also analyzed by changing the thickness parameters in the tables.

Table 7: Theoretical resonant frequencies (in MHz) for an air-gap tuned structure, a=10cm, ε_{r2}=2.32, h_2=1.59mm.

Mode	$f_{r,nm}$ h_1=0	$f_{r,nm}$ h_1=0.5mm	$f_{r,nm}$ h_1=1.0mm
TM_{10}	1278	1436	1509
TM_{11}	2224	2486	2613
TM_{20}	2556	2871	3018
TM_{21}	3398	3798	3992
TM_{30}	3834	4307	4526

Another study is done by D. Guha and J. Y. Siddiqui in [5].The geometry is defined in figure 12.

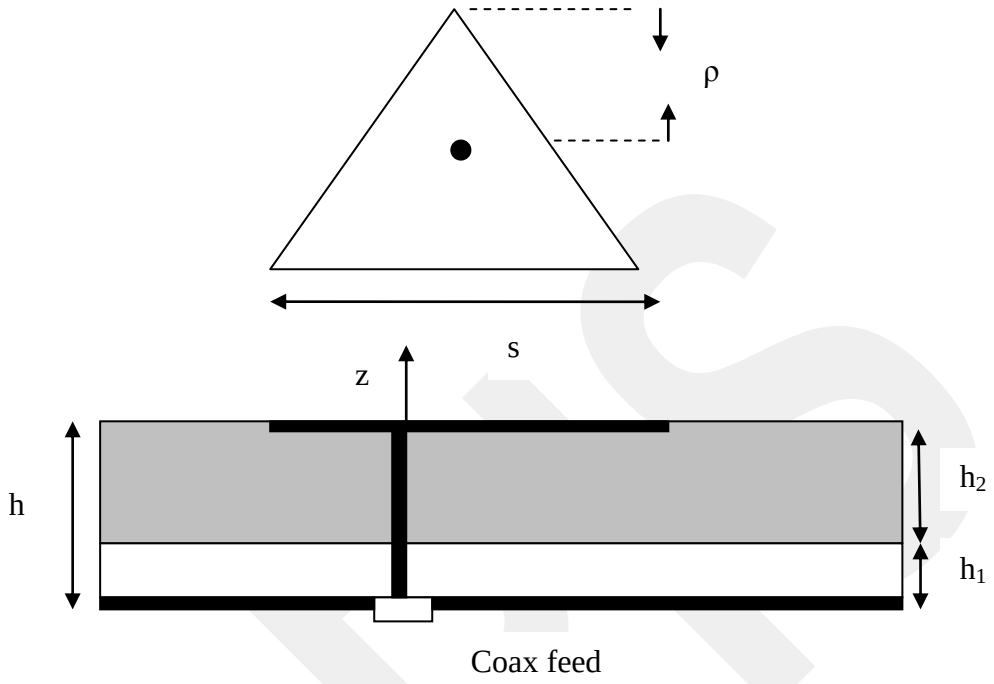

Figure 12: Coax-fed Equilateral Triangular Microstrip Patch (ETMP) antenna with an air-gap between the substrate and the ground plane [5].

The resonant frequency in this study is defined as:

$$f_{r,nm} = \frac{2c}{3s_{eff}\sqrt{\varepsilon_{r,eff}}}(n^2 + nm + m^2)^{\frac{1}{2}} \quad (24)$$

where c is the velocity of light in free space, s_{eff} is the effective side-length of an ETMP (Equilateral triangular microstrip patch), and $\varepsilon_{r,eff}$ is the effective relative permittivity of the medium below the patch. In the present formulation, s_{eff} and $\varepsilon_{r,eff}$ are determined using the improved cavity model [26]. The parameter $\varepsilon_{r,eff}$ is derived in terms of ε_{re} and $\varepsilon_{r,dyn}$ where ε_{re} is the equivalent permittivity of the two-layer dielectric medium and $\varepsilon_{r,dyn}$ is the dynamic dielectric constant of the medium below the patch. The quantity $\varepsilon_{r,dyn}$ of an ETMP can be obtained from the

static main and static fringing capacitances of an equivalent circular microstrip disk [26].

The equivalent circle of an equilateral triangular patch is determined based on equal circumference of both the triangle and circular patch, which counts the fringing field effects for the dominant modes. The radius of an equivalent circle thus can be equated as:

$$a = \frac{3}{2\pi} s \tag{25}$$

The comparison of the study is presented in the tables below with corresponding errors.

Table 8: Comparison of measured and normalized theoretical resonant Frequencies for low permittivity value, a=100mm, ρ=3.0mm, ε_{r2}=2.32, h_1=0, h_2=1.59mm.

Mode	**Resonant frequency (MHz)**			
	[13]	**[5]**	**[22]**	**[10]**
TM_{10}	1288	1285	1281	1280
TM_{11}	2259	2226	2219	2242
TM_{20}	2610	2570	2562	2550
TM_{21}	3454	3400	3389	3400
TM_{30}	3875	3855	3843	3824
Average error %		1.0	1.4	

The resonant frequencies of the antennas are determined via different methods and the experimental results are presented in the tables 8 and 9. The error obtained from these two antennas was 1.4% and 1.2%.

Table 9: Comparison of measured and normalized theoretical resonant Frequencies for low permittivity value, a=41mm, ρ=5.0mm, ε_{r2}=10.5, h_1 =0, h_2=0.7mm.

Mode	Resonant frequency (MHz)			
	[13]	**[5]**	**[22]**	**[13]**
TM_{10}	1522	1516	1501	1519
TM_{11}	2654	2626	2601	2637
TM_{20}	3025	3032	3003	2995
TM_{21}	4038	4011	3972	3973
TM_{30}	4518	4548	4504	4439
Average error %		0.6	1.2	

The next study is done by D. Karaboğa, K. Güney, N. Karaboğa, and A. Kaplan [22]; Simple expression of effective side-length is developed to get resonant frequency of an equilateral triangular microstrip antenna. It is obtained by using a modified genetic algorithm. Good agreement achieved the experimental results and the studies in the literature.

$$f_{mn} = \frac{2c}{3a(\varepsilon_r)^{\frac{1}{2}}}[m^2 + mn + n^2]^{\frac{1}{2}} \tag{26}$$

$$a_{eff} = a + h(1.2 + \frac{2.25}{\sqrt{\varepsilon_{eff}}}) \tag{27}$$

$$\varepsilon_{eff} = \frac{1}{2}(\varepsilon_r + 1) + \frac{1}{2}(\varepsilon_r - 1)(1 + \frac{12h}{W_{equ}})^{-\frac{1}{2}} \tag{28}$$

$$W_{equ} = \frac{3^{0.25} a}{2} \tag{29}$$

$$f_{mn} = \frac{2c}{3a_{eff}\,(\varepsilon_{eff})^{\frac{1}{2}}} [m^2 + mn + n^2]^{\frac{1}{2}} \tag{30}$$

A well agreement is done with the results obtained by simple genetic algorithm with using the formulas stated and it is compared with the results indicated literature. Around 273 MHz large error is obtained. It is also underlined that the mathematical formula, which is used to determine resonant frequency in this study, is not complicated. Simple and accurate calculation is performed in this study.

One study is done by N. Kumprarsert and K. W. Kiranon that is defined and presented with the results and comparison in [9].

An approximate solution of the capacitance of circular microstrip patch to account for fringing field is used to calculate the resonant frequency of an equilateral triangular patch antenna.

The region between the microstrip and ground plane treated as a cavity bounded by magnetic walls along the edges and by electric walls from above and below. The fringing fields are also taken into account. As in several studies [27], [28] the resonant frequency calculation is based on the effective radius of a circular disk, depends on the radius of the disk a and dielectric thickness h , and is given as:

$$a_e = a[1 + \frac{2h}{\pi \varepsilon_r a}\left\{\ln\left(\frac{\pi a}{2h}\right) + 1.7726\right\}]^{\frac{1}{2}} \tag{31}$$

The formulation of a_e modified in 1984 by Y. Suzuki and T. Chiba as:

$$a_{eff} = a_{eq}[1 + \frac{2h}{\pi a_{eq}\,\varepsilon_r}\left\{\ln\left(\frac{\pi a_{eq}}{2h}\right) + 1.7726\right\}]^{\frac{1}{2}} \tag{32}$$

The original triangular patch area is defined as s and the a_{eq} is formulated as:

$$a_{eq} = \sqrt{\frac{s}{\pi}} \tag{33}$$

Therefore, the a_{eff} equation yields the eqn. 34 as:

$$a' = a[1 + \frac{2h}{\pi a_{eq}\,\varepsilon_r}\left\{\ln\left(\frac{\pi a_{eq}}{2h}\right) + 1.7726\right\}]^{\frac{1}{2}} \tag{34}$$

Effective dimension is estimated using the capacitance formula as:

$$c = \frac{a^2\pi\varepsilon_r\varepsilon_0}{h}[1 + \frac{2h}{\pi\varepsilon_r a}\left\{\ln\left(\frac{a}{2h}\right) + (1.41\varepsilon_r + 1.77) + \frac{h}{a}(0.268\varepsilon_r \tag{35}$$

The equation of a_{ef} (effective length of triangular patch) which depends on a (physical length of triangular patch) reduces to eqn. 36:

$$a_{eff} = a[1 + \frac{2h}{\pi a\varepsilon_r}\left\{\ln\left(\frac{a}{2h}\right) + (1.41\varepsilon_r + 1.77) + \frac{h}{a}(0.268\varepsilon_r + 1.65\right\}]^{\frac{1}{2}} \tag{36}$$

Therefore, the resonant frequency of the equilateral triangular patch is defined as:

$$f_{m,n,l} = \frac{2c}{3a_{ef}\,(\varepsilon_r)^{\frac{1}{2}}}[m^2 + mn + n^2]^{\frac{1}{2}} \tag{37}$$

The resonant frequencies calculated by using the formula presented in [9] are compared with the results of [11] - [27] - [28] and good agreement is achieved with the measured values. The detailed results are stated as in the following table.

Table 10: Resonant frequencies (in MHz) of an equilateral triangular patch antenna, a=10cm, ε_{r2}=2.32, h_2=1.59mm.

Mode	Measured (GHz)	Calculated (MHz)			
		[27]	[28]	[10]	[9]
$\mathbf{TM_{1,0,-1}}$	1280	1273	1273	1299	1289
$\mathbf{TM_{1,1,-2}}$	2242	2239	2205	2252	2233
$\mathbf{TM_{2,0,-2}}$	2550	2546	2546	2599	2579
$\mathbf{TM_{2,1,-3}}$	3400	3419	3369	3439	3411
$\mathbf{TM_{3,0,-3}}$	3824	3819	3820	3899	3868

[43] is done for correction of the resonant frequency values determined for the patch properties $a = 10cm, \varepsilon_r = 2.32, h = 0.159cm$ and the results are presented which is obtained with the correction.

A Study is done by W. Chen, K. F. Lee, and J. S. Dahele [24]. The study contains comparison of the previous experimental data of Dahele and Lee with moment method results. New measurements moment method results for $\varepsilon_r = 10.5$ and comparison with Gang's hypothesis are presented. Verification of the relationship among the various modes by measurements and by moment method is mentioned. A curve fitting formula yielding the resonant frequency of the lowest mode, which is within 1% of the value obtained from moment method analysis, is also presented. The geometry of the probe-fed equilateral triangular microstrip antenna is shown in Figure. 13.

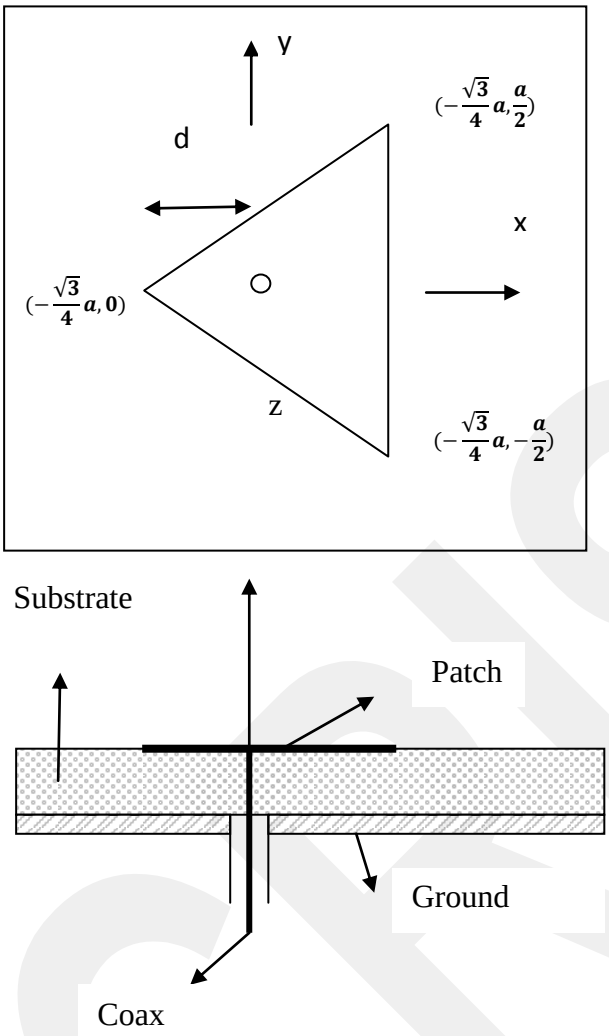

Figure 13: The geometry of an equilateral triangular patch drawn as in [13].

Spectral domain full wave analysis and the moment method are used to analyze the resonant frequency. Although the analyze method does not the same as the method defined in this thesis the results will be useful to compare the ones that is mentioned in this study. In the study [13] source-free case is considered and a procedure similar to rectangular patch is employed. By enforcing the boundary condition that the tangential electric field vanishes on the patch, and applying Galerkin's method, the matrix equation is founded as in eqn.38:

$$[A_{ij}][C_n] = 0 \tag{38}$$

Moreover, A_{ij} and J_n formulated as in eqn. 39 and eqn.40:

$$A_{ij} = \frac{1}{(2\pi)^2} \iint_{-\infty}^{\infty} [Z_{xx} \tilde{f}_{ix}\, \tilde{f}_{jx}(-k_x, -k_y) + Z_{xy}\left(\tilde{f}_{iy} \tilde{f}_{ix}(-k_x, -k_y) + \tilde{f}_{ix} \tilde{f}_{jy}(-k_x, -k_y)\right) + Z_{yy}\left(\tilde{f}_{iy} \tilde{f}_{iy}(-k_x, -k_y)\right)] dk_x dk_y \quad (39)$$

$$\vec{J}_s = \sum C_n \, (f_{nx} \hat{x} + f_{ny} \hat{y} \quad (40)$$

Here ~ denotes Fourier transform and $\vec{J}_s$ is the surface density on the patch. The matrix elements, Z_{xx} , Z_{xy} and Z_{yy} defined in literature and complex resonant frequency $(f_r + jf_i)$ is found by solving the equation $\det(A_{ij}) = 0$

The results obtained from the [13] compared with the results obtained from [7], [22], [23] and [24] both calculated and measured values have good agreement for different modes and thickness.

K. Güney [29] presents few formulas and the results obtained from these formulations. The comparison and results are listed by tables for different modes. The resonant frequency is defined in [29] as in various studies as:

$$f_{mn} = \frac{2c}{3a(\varepsilon_r)^{\frac{1}{2}}} [m^2 + mn + n^2]^{\frac{1}{2}} \quad (41)$$

It is mentioned that the effective side-length replaces the side-length in [29] as determined in [11] as:

$$a_{e1} = a + \frac{h}{\sqrt{\varepsilon_r}} \quad (42)$$

The relative permittivity also is replaced with the effective permittivity in [29] as in [7] so the effective permittivity is expressed as:

$$\varepsilon_{eti} = \frac{1}{2}(\varepsilon_r + 1) + \frac{1}{2}(\varepsilon_1 - 1)\alpha_{ti} \tag{43}$$

The parametersα_{ti}, $W(x)$ and H are defined as the eqns. 44, 45, and 46:

$$\alpha_{ti} = \frac{1}{H}\int_0^H [1 + \frac{12h}{W(x)}]^{\frac{-1}{2}} dx \tag{44}$$

$$W(x) = \frac{2\pi}{\sqrt{3}} \tag{45}$$

$$H = \frac{\sqrt{3}a}{2} \tag{46}$$

By substituting the formulas, the α_{ti} reduces to a form as in eqn.47 and the $A = 6\sqrt{3}h$ equation is given:

$$\alpha_{ti} = \frac{[\sqrt{(A+H)H} - AL_n(\sqrt{H} + \sqrt{H+A})]}{H} + \frac{Aln(A)}{2H} \tag{47}$$

The [29] suggests changing side-length with a closed-form expression as:

$$a_{e2} = a + \frac{h^{0.6}a^{0.38}}{\sqrt{\varepsilon_r}} \tag{48}$$

This new expression fit with the measured and theoretical data in the literature and detailed results mentioned in [29].

The study [12] had done by R. Garg and S. A. Long gives the results of the measured resonant frequency of an equilateral triangular patch antenna with side-length 10cm, thickness 0.159 cm and relative permittivity 2.32. The effective radius and the effective dielectric permittivity are also mentioned for different modes. The resonant frequency formulation is used as in other studies and the effective radius expression

is used for finding the resonant frequency. It is also state that the sum of the mode coefficients m, l and n must be zero.

The study of Xu, expresses the general form resonant frequency expression, which is based on the average value of effective dielectric constant [7]. The cavity model is used to analyze in this paper and it is stated that since a perfect magnetic wall does not exist for a practical microstrip patch antennas, the computed resonant frequencies using the cavity model should be corrected in some way. In the literature these correction is done by correcting the side-length and permittivity expression. The studies show that for correction, the effective relative permittivity is used instead of relative permittivity and effective side-length is used instead of side-length expressions. The expressions are formulated as in eqns.49 and 50:

$$a_{eff} = a + \delta a \tag{49}$$

$$\varepsilon_e = \frac{(\varepsilon_r + 1)}{2} + [\frac{(\varepsilon_r - 1)}{2}]\alpha \tag{50}$$

a is the physical dimension, a_e is effective dimension, E_r is relative dielectric constant, E_e is effective dielectric constant, δ_a is the dimensional correction factor and α is the permittivity correction factor (PCF). The PCF for antennas α_{tl} is obtained by a linear average procedure as in [30]. In the procedure, the effective permittivity E_{eti} of the ETMA is calculated from the average value of the effective permittivity for strip widths W = 0 and W = a as:

$$\begin{aligned} \varepsilon_{eti} &= \frac{[\varepsilon_e(W = 0) + \varepsilon_e(W = a)]}{2} \\ &= \frac{(\varepsilon_r + 1)}{2} + \frac{(\varepsilon_r - 1)}{4}(1 + \frac{12h}{a})^{-\frac{1}{2}} \end{aligned} \tag{51}$$

$$\alpha_{tl} = \frac{(1 + \frac{12h}{a})^{-\frac{1}{2}}}{2} \tag{52}$$

$$\alpha_{tl} = \frac{1}{H}\int_0^H (1 + \frac{12h}{W(x)})^{-\frac{1}{2}} dx \tag{53}$$

$$W(x) = \frac{2x}{\sqrt{3}} \tag{54}$$

$$\varepsilon_{eti} = \frac{(\varepsilon_r + 1)}{2} + \frac{(\varepsilon_r - 1)}{2}\alpha_{tl} \tag{55}$$

$$\alpha_{ti} = \frac{\left[\sqrt{(A+H)H} - Aln(\sqrt{H} + \sqrt{H+A})\right]}{H} + \frac{Aln(A)}{2H} \tag{56}$$

$$A = 6\sqrt{3}h \tag{57}$$

$$H = \frac{\sqrt{3}a}{2} \tag{58}$$

By using the given formulations, the resonant frequency of an equilateral triangular microstrip patch is found in this paper as in eqn.59, which is a function of effective side-length a_e that is expressed in eqn. 60:

$$f_{m,n,l} = \frac{2c}{3a_e(E_{eti})^{\frac{1}{2}}}[m^2 + mn + n^2]^{\frac{1}{2}} \tag{59}$$

$$a_e = a + \frac{h}{\sqrt{\varepsilon_r}} \tag{60}$$

The formulations are done for generalize the resonant frequency formulation and are implemented for ETMA. It is obtained that the results have good agreement with the measured and calculated values of resonant frequency existing in literature. It is

concluded that the integration average method is conceptually reasonable, and it provides better correction for the resonant frequencies of microstrip antennas. It is concluded that the procedure can be easily applied to the arbitrary shaped MA (Microstrip Antenna) as applied to the ETMA (Equilateral Triangular Microstrip Antenna) in [7]. Nasimuddin, Karu Essele and A.K. Verma do another approach in [31]. In spite of several studies that find the effective side-length of the equilateral triangular patch by replacing with a circle this study, assume that rectangular patch exchange will be better to count the fringing field effects. The geometry is drawn as in figure 14.

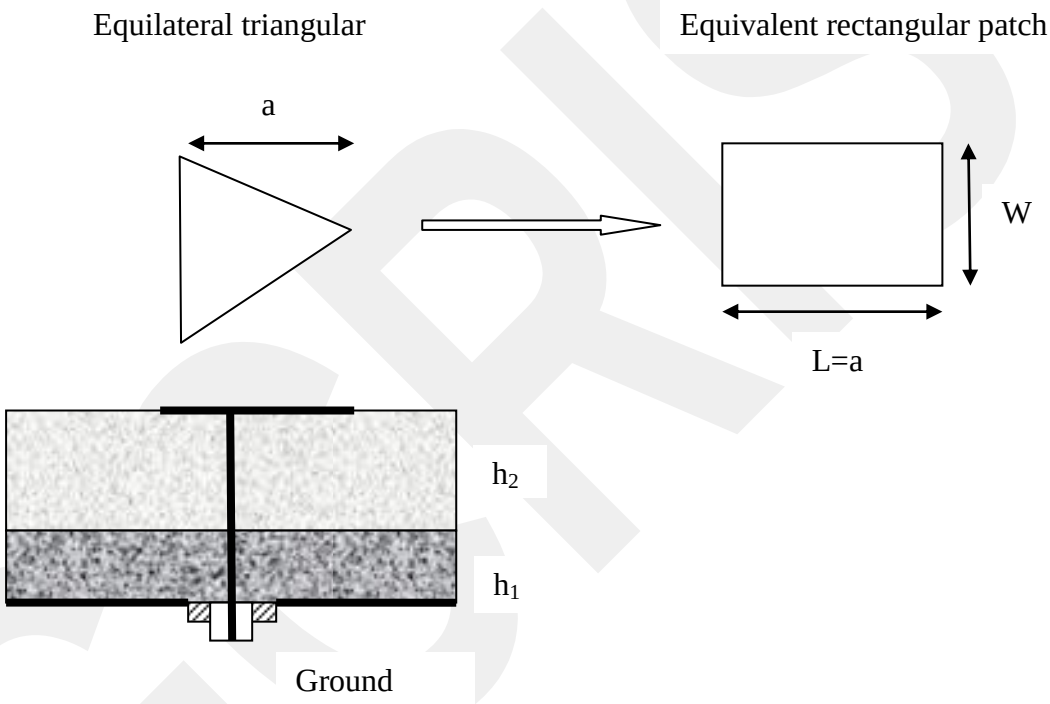

Figure 14: Replacement of a triangular patch with a rectangular patch [31] .

It is stated that several studies is done for finding resonant frequency of a equilateral triangular patch since it has smaller size and similar radiation characteristics with the rectangular microstrip antennas. There are two models proposed in this study. The models separate each other with the expression of the effective side-lengths. In the first model proposed the side-length a is replaced by effective side-length a_{eff} and ε_{req} is replaced by the average complex effective relative permittivity $\varepsilon^*_{r,eff}$ under the patch. Curve-fitted formula of effective side-length is given as:

$$a_{eff} = a + h(0.01 + (\frac{D(\varepsilon_r)}{\sqrt{\varepsilon'_{r,eff}}}) \quad (61)$$

In the eqn. 61, the parameter $D(\varepsilon_r)$ is the permittivity dependent parameter expressed by the empirical relation as:

$$D(\varepsilon_r) = \begin{cases} 4.08 & ; \varepsilon'_{req} \geq 2.2 \\ 3.5709 - 0.8591 * \varepsilon'_{req} + 0.3469 * \varepsilon'^{2}_{req}; \varepsilon'_{req} \leq 2.2 \end{cases} \quad (62)$$

ε'_{req} and $\varepsilon'_{r,eff}$ are the respective real values of the homogenous relative permittivity of medium below the patch and the relative permittivity of the equilateral triangular patch and the average effective relative permittivity of the equivalent rectangular patch from both and length sides. If there is no air-gap in the structure, the relation between effective and relative permittivity is expressed as:

$$\varepsilon^*_{req} = \varepsilon^*_{r2}\varepsilon^*_{r,eff} \quad (63)$$

$\varepsilon^*_{r2}\varepsilon^*_{r,eff}$ denotes the complex average effective relative permittivity of the equilateral triangular microstrip patch antenna. So the effective conjugate of the permittivity is formulated as:

$$\varepsilon^*_{r,eff} = \frac{\varepsilon^*_{r,eff} + 1}{2} + \frac{1}{2}\left(\frac{\varepsilon^*_{req} - 1}{2}\right)(1 + \frac{10h}{W}) \quad (64)$$

The second model computes the effective length of the equilateral triangular patch from the equivalent rectangular patch as:

$$a_{eff} = a + \left[\frac{(W_{eq} - W)}{2}\right][\frac{Re(\varepsilon^*_{r,effw}) + 0.3}{Re(\varepsilon^*_{r,effw}) - 0.258}] \quad (65)$$

Here W_{eq} is the equivalent width, which is obtained from the planar waveguide model, $\varepsilon^*_{r,effw}$ is the complex effective relative permittivity computed from side-length from the side width of the equivalent rectangular patch formulated by eqn.66:

$$W_{eq} = \frac{120\pi h}{z(W)\sqrt{Re(\varepsilon^*_{r,effw})}} \quad (66)$$

To conclude up in [31] good agreement is achieved with the measured results in both proposed models. It is mentioned that models have accuracy within 0.7% as compared with the measurements.

3.2 Literature Review for Dual-Frequency Equilateral Triangular Patch

As mentioned in introduction there are several applications for dual-frequency antennas that is studied in literature. Since there are, only several studies on calculating the operational frequencies of dual-frequency antennas, a few papers will be presented in literature review. Section 3.2 will demonstrate the past studies and will be an aggregation of results that will compared with the theory obtained from section 5.1.1.

3.2.1 Methods to form dual-frequency microstrip antennas

To obtain dual band, a few attempts have been made [34] - [45] in the literature. Dual frequency operation of an equilateral triangular patch antenna is demonstrated by using tunable slot-loaded patches [33] and using stacked patches [34]. Moreover, using a pair of spur lines [36] and using a slit [37] are other ways to obtain dual-band. Using a V shaped slot [38], loading two pair of narrow slots in the triangular patch [39] and [40] and using shorting pins [37],[38],[41], [44],[45] are the other attempts to form dual-band operations.

3.2.1.1 Shorting-pin loaded microstrip antennas and their results

Miniaturization of the patch antenna is one of the aims in wireless communication systems. Using large permittivity substrate is one of the techniques for size reduction although this has a negative impact on impedance bandwidth. Use of a shorted patch can be another solution to provide small size. The studies presented in literature that are done to provide dual-frequency patch antenna and miniaturization showed that

inserting shorting-pin is one of the best method. A conducting pin is used to form a dual-frequency patch antenna. It is stated that shorting pin-loaded patch antennas have reduced size.

These kinds of antennas have low cross sections so they have advantages on other antennas in some systems like satellite positioning systems. It is also mentioned that a shorting pin-loaded microstrip antennas, which are used in low frequency communication systems are suitable for these kinds of systems since they have low profile and small size. Although the shorting pin-loaded patch antennas are preferable choice the literature is short of detailed theoretical results. Mostly the studies are based on the experimental results, measurements, and numerical methods.

The presented studies showed that inserting shorting pin might cause some manufacturing difficulties since the feed position is close to the position of the shorting pin in a range measured in terms of millimeters. However, this method is determined as simple and achieves high performance. Using shorting pin is a challenging method. It yields frequency ratio tuning. By changing the position of the feed, the frequency tuning is achieved in various studies.

A demonstrated study [46] that is based on an analysis of a circular-disk microstrip antenna uses cavity model solution and compares the results with HFSS results. It is indicated that the circular disk patch antenna design is near to maturity so a different model is presented in this paper. The model has a conducting pin at the centre of the geometry, which makes the patch shorted. The calculated values are compared with the results of HFSS design, and it is obtained that the formulas presented in the proposed study has enough accuracy.

An investigation is done, which is based on cavity model in [47]. The proposed study gives theoretical analysis method for shorting pins loaded rectangular microstrip patch antenna. The patch is shorted with a single shorting pin and two shorting pins separately. The results are obtained for both conditions with the calculation and optimization technique. It is concluded that single shorting pin provides narrower bandwidth. The study is extended to multiple number of shorting pin-loaded rectangular patch.

Notch loaded half disk patch is demonstrated in [48]. The importance of the bandwidth increment is mentioned. Several approaches are stated to increase the bandwidth of the patch antenna. Increasing the substrate thickness, incorporating multiple resonances, and using multiple-layers are stated as the ways of increasing the bandwidth. Miniaturization of the antenna was another topic that the authors stressed. Using high permittivity substrate and short-circuited post or shorting pin were two the methods that are used to miniaturize the patch. A notch and a shorting pin-loaded half disk patch is presented and analyzed in the study and return loss-frequency relations are presented with several figures. It is concluded that the bandwidth of the patch antenna depends on the length of the notch, shorting pin and gap spacing.

The studies presented in the literature mentions that dual-frequency applications are increasingly popular. There are various methods to provide dual frequency antenna such as slot-loaded, stack-loaded, and notch-loaded antennas but the most preferable one is shorting post and shorting pin-loaded patch antennas. Shorting pin usage increases the performance and can be assumed as a simple application. The studies showed that shorting pin reduces antenna size in all shapes of antennas. It also provides dual frequency applications. The position variation of the shorting pin allows frequency tuning for the designer. Ratio of the upper operating to the lower operating frequency is an important task for designer that changes application to application. In some applications, higher frequency ratio is desired. The frequency ratio reaches its maximum value at a shorting pin position that is closer to the tip of the patch. It should be also considered that manufacturing tolerance increases if the distance between feed position and the shorting pin position increases.

The studies showed that frequency ratio is higher in triangular patch compared to the other shapes. According to this advantage, equilateral triangular patch antenna with shorting pin is investigated in next section. The parameters effects the upper and lower frequency analyzed. The permittivity and shorting pin position impacts are summarized with the proposed studies in the literature.

3.2.1.1.1 Shorting-pin loaded equilateral triangular patch antennas presented in literature and their results

There are various studies demonstrated in literature that is done for determining the operating frequencies of a shorting pin-loaded equilateral triangular patch antennas and indicating the frequency ratios of these antennas. As far as author knows, there is no study to compute resonance frequency of a shorting pin-loaded dual-frequency equilateral triangular patch antenna by using cavity model analysis. Most of the studies present measured values of the operating frequencies [41], [44], [45] and [41].

A shorting pin-loaded dual-frequency triangular and rectangular microstrip antenna is presented and discussed in [41]. The operating frequencies are measured in TM_{10} mode. The frequency ratios are analyzed for both rectangular and triangular patch. The first design applied to a rectangular patch as in figure 15. As drawn in figure 15, *W* is width of the patch where *L* is the length of the rectangular patch. There is a substrate layer with a relative permittivity ε_r under the patch, which has a thickness *h*. Distance from the tip of the rectangular patch to the shorting pin position is determined as *ds*. Moreover, the patch is fed with a coax probe.

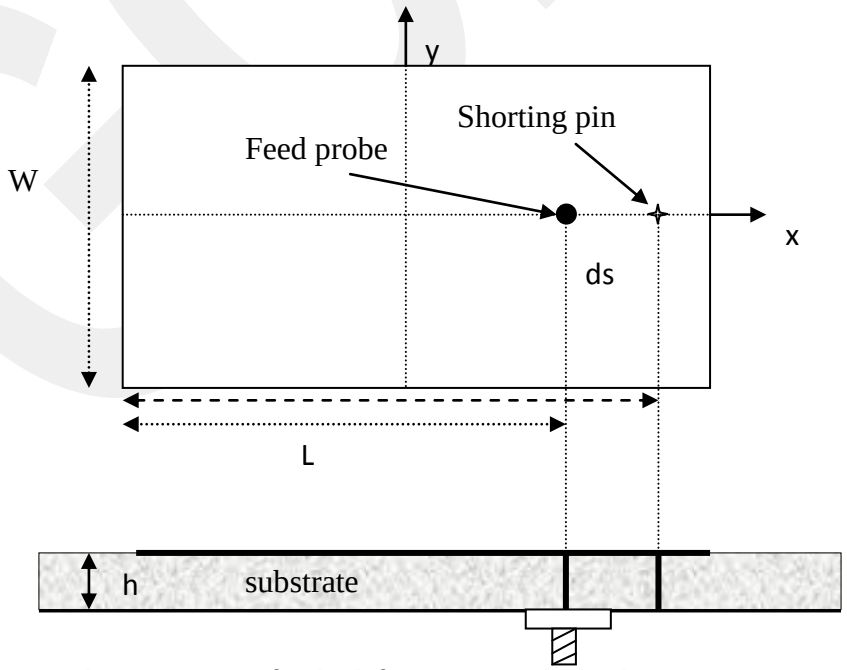

Figure 15: The geometry of a dual-frequency rectangular microstrip antenna with a shorting pin [41].

The parameters of the rectangular antenna drawn in the figure above is determined as; Permittivity of the substrate is 4.4, the thickness is 0.762mm, *L*=37.3mm and *W*=24.87mm. The upper frequency varies between 1900-2310MHz, where the lower frequency varies between 722-950MHz. The frequency ratio is increased to 3.2 from frequency ratio 2. The frequency characteristics with respect to pin position is indicated and it is observed that the lowest upper frequency and the highest lower frequency occurred in a pin position ratio in between 0.4-0.6.The frequency ratio ($f_{r,upper}$ / $f_{r,lower}$) reached to 3.2 when the pin position side-length ratio become u=1.

The second design is a shorting pin-loaded equilateral triangular antenna. The designed triangular patch is drawn as in Figure 16.

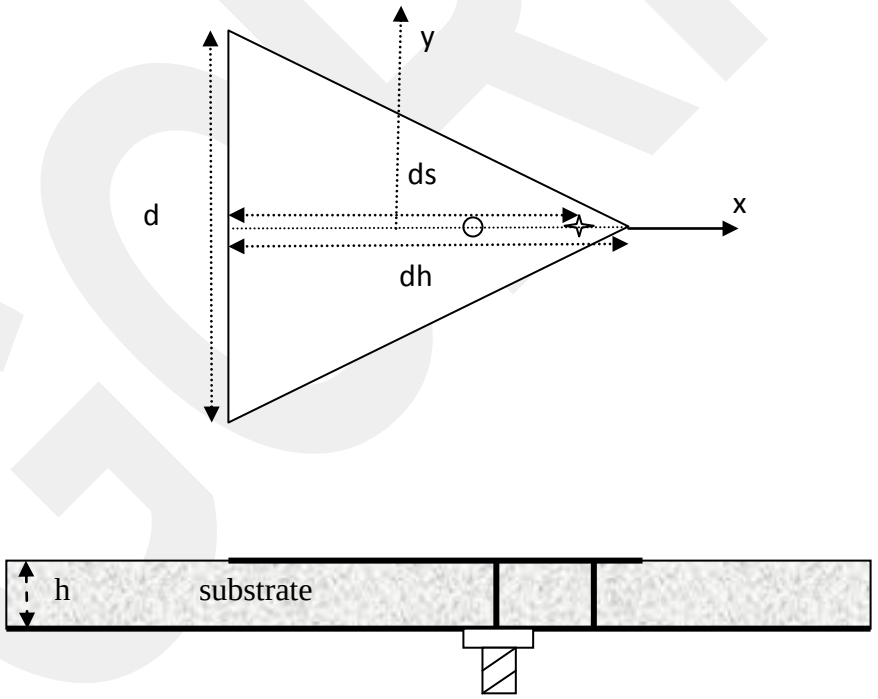

Figure 16: The geometry of a dual-frequency triangular microstrip antenna with a shorting pin.

In the figure, *d* is the side-length of the triangular patch and *dh* is the distance from the top of the triangular to the bottom side-length where *ds* is the shorting pin

distance from the tip of the triangle. In this geometry, substrate with a permittivity ε_r and a thickness *h* is design for the triangular patch. The patch is fed by coax feed.

The parameters of the equilateral triangular antenna is drawn in the figure above and are determined as the permittivity of the substrate is 4.4, the thickness is 0.762mm and the side-length is equal to 50mm.

Upper and lower frequencies are also measured for the triangular patch. The frequency ratios are studied. It is observed that the frequency ratio varies between 2.5-4.9. The highest lower frequency (766MHz) and the lowest upper frequency (1886MHz) are observed at a pin position ratio to distance of the tip of the triangular to the bottom side (*ds/dh*) 0.33. The null voltage point is at the *ds/dh* =0.33.The frequency ratio at the null voltage point is measured as 2.5.

The *ds* to *dh* ratio is increased to 1 and the frequency ratio is reached at 4.9. The upper frequency is measured as 2276MHz, and the lower frequency is measured as 464MHz at this ratio.

It can be concluded that triangular microstrip patch provides larger frequency ratio in similar designs of other microstrip shapes. So according to the design requirements, the patch parameters should be checked and the triangular patch should be chosen if more frequency ratio is desired.

[44] is one of the studies that is presented by Kin-Lu Wong and Shan Cheng Pan. An experimental research is demonstrated in this study, and the results are discussed. A shorting pin-loaded equilateral triangular patch antenna is proposed and its geometry is drawn as in the figure 17.

The geometry shows one layer-shorting pin-loaded triangular microstrip patch antenna with a side-length *d* and the substrate has a thickness *h*. The distance to shorting pin and probe feed is determined as *ds* and *dp* respectively.

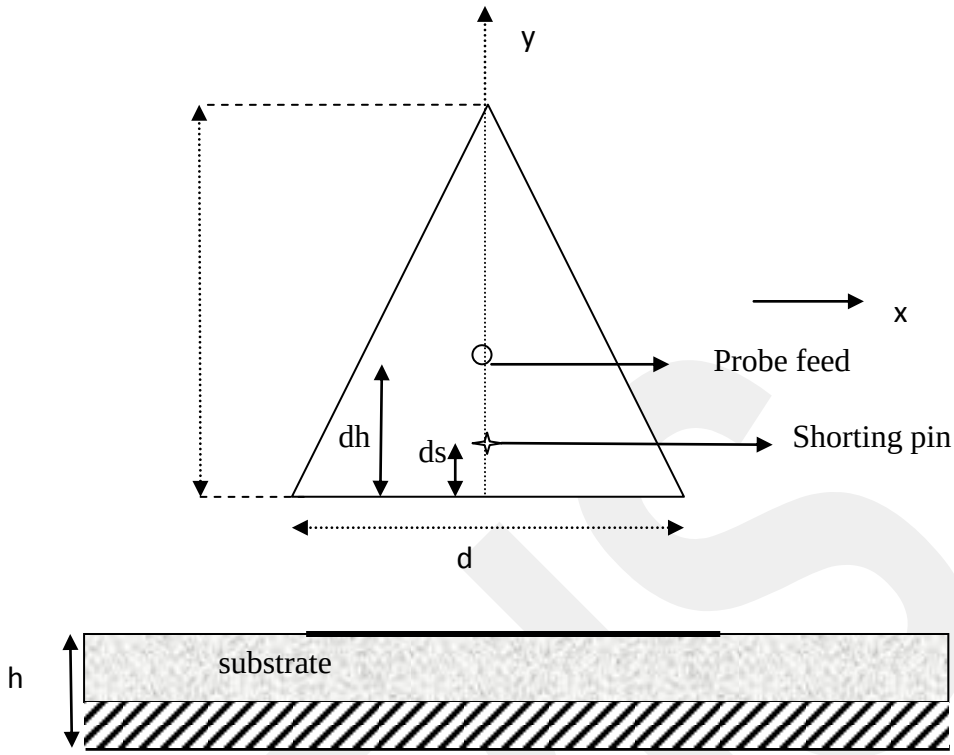

Figure 17: Geometry of compact triangular microstrip antenna.

The study informs about the microstrip antenna technology and its incrementally increasing usage in wireless communication systems. The importance of loading a shorting pin to a triangular patch antenna is also mentioned in the presented paper. It is stated that loading a shorting pin significantly reduces the antenna size. Experimental values are presented for the given triangular patch at TM_{10} mode, the results are discussed. In addition, comparison of a compact with a conventional microstrip antenna is done.

At a given operating frequency, the required patch dimension is significantly reduced, and the reduction in the patch is limited by the distance between null voltage point in the patch and patch edge [44]. Therefore, if the shorting pin-loaded triangular patch compared to the shorting pin-loaded rectangular and circular patch, it is expected that an equilateral triangular microstrip patch have a smaller size. An equilateral triangular microstrip patch is excited at its fundamental mode where the null-voltage point is at two thirds of the distance from the triangle tip to the bottom side of the triangle, can have a much larger reduction in the resonant frequency,

when applying the shorting-pin loading technique[44]. So [44] is done for verifying these information and discusses the study with the results.

The antenna parameters are given as d=59.9mm, h=0.762 and permittivity $\varepsilon_r = 3.0$ and measurements are done for the given antenna. Lower frequencies of the given antenna is presented which is related to ratio of the shorting pin position and the distance between tip of triangle and the one side of the triangle (*ds/dh*). Return loss and upper frequency are also presented for given *ds*=13.25mm.

The lower frequency varies between 410-780 MHz for the ratio values (*ds/dh*) between 0-1. Maximum value of the lower frequency is measured at a ratio=0.33 where the null voltage occurs. The lower frequency becomes its minimum value at a ratio=1 which has a value 410MHz. It is stated that this value is only about the %22 of the conventional triangular microstrip antenna without a shorting pin. The upper frequencies of the compact and conventional triangular microstrip antenna are measured as 1970MHz and 1930MHz, respectively. The return loss decreases to approximately -23dB at a frequency 1930MHz.

The result showed that the null voltage occurs at *ds/dh*=0.33 and there is a size reduction. The compact triangular microstrip patch is almost <5% of a conventional triangular patch antenna. With a simple approximate calculation, the frequency ratio increases to 4.7.

The study about shorting pin-loaded triangular microstrip patch antennas shows significant experimental results, as discussed in [42]. A design of a shorting pin-loaded triangular microstrip antenna is presented in the study. Large tunable frequency ratio is achieved by changing the pin position. The frequency ratio is ($f_{r,upper}$ /$f_{r,lower}$) varied between 2.5 to 4.9 for different shorting pin positions. Experimental results are demonstrated and discussed in this study. The geometry of the presented antenna is the same as the antenna geometry presented in [44].

The importance and the popularity of the dual-frequency microstrip antennas are underlined. It is stated that there are several designs that are demonstrated in literature that considers the frequency ratio and most of the designs have limited

frequency ratio, being in between 1.3-2. As mentioned before, the frequency ratio can be increased by adding some other circuitry like varactor diodes, shorting pins, slots etc. A shorting pin is loaded to microstrip antenna in this study to form a dual-frequency microstrip antenna.

The antenna presented in the study has a permittivity=4.4, thickness=1.6mm and side-length=50mm. Graph of the frequency ratios, upper and lower operating frequencies with respect to shorting pin position is drawn in the paper. The graph summarizes the results. The upper frequency varied in between 1700MHz to 2400 MHz where the lower frequency changes in between 450MHz to 800 MHz. The frequency ratio remains in between 2.5 and 4.9.

Null voltage point occurs at the ratio of 0.33 as it is already mentioned in other studies presented in literature. The maximum value of the frequency ratio is 4.9 where the minimum value is 2.5. A comparison is done with a rectangular patch and it is concluded that the frequency ratio of a triangular patch is much greater than a rectangular patch, which has a ratio in between 2.0 and 3.2. It is underlined that triangular microstrip antennas are more useful for various applications than other shapes since it has large frequency ratio. The maximum frequency ratio is achieved at ds/dh=1.0 which is approximately 4.9. At this position, the return loss of the patch is given and stated that the lower frequency is 464 MHz where the upper frequency is 2276 MHz. It is concluded that this kind of designs are suitable for various applications like SAR (synthetic aperture radar) systems.

Another study is presented and as far as authors know this is the only study that calculates the operating frequencies and impedance [45]. The study presents a shorting pin-loaded equilateral triangular patch. The shorting pin positions are taken into account and the transmission line model is used to analyze the operating frequencies. The relations between shorting pin positions, permittivity, and operating frequencies are demonstrated.

The geometry of the antenna presented antenna is defined as in figure 18;

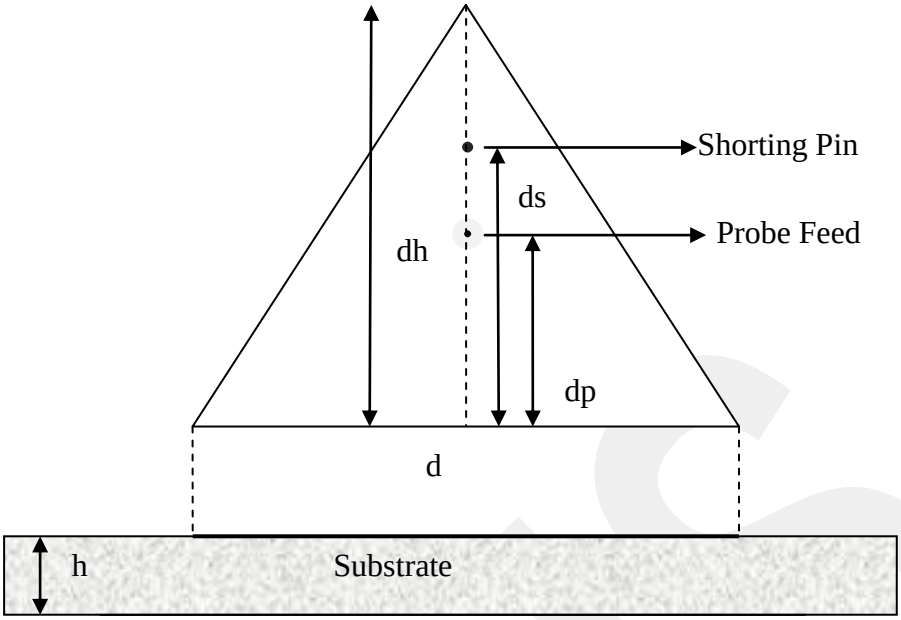

Figure 18: Top and side view of the shorting pin-loaded equilateral triangular patch.

The upper and the lower frequencies of the patch are calculated with the transmission line model that is presented in this study. The results are compared with the experimental values. For ds/dh= 0 the experimental value of the upper frequency is 2GHz where the transmission line model calculation is equal to 2.2 GHz at the same pin position. Experimental value of the lower frequency is measured 0.6 GHz where the transmission line model gives 0.8 GHz. The maximum lower frequency and the minimum upper frequency are obtained at a ratio ds/dh=0.33. This point is named as null-voltage point.

A frequency ratio (FR), which is the ratio of the upper frequency to the lower frequency, is determined. The FR and *dh/ds* characteristics are analyzed and the shorting pin position effect on the frequency ratio is analyzed. Minimum frequency ratio is occurred at null-voltage point. By various experimental results, it is concluded that the minimum frequency ratio decreases if the substrate permittivity increases. In the presented conditions, the frequency ratio is varied from 2.81-1.68 for permittivity values of 1.0 to 9.8. Frequency ratio depends on the distance between null voltage point and the shorting pin position. The frequency ratio increases if the distance between null voltage point and shorting pin position increase.

Based on this relation, the maximum frequency ratio is obtained when the shorting pin is placed at the tip of the triangular patch. Maximum frequency ratio decreases if the substrate permittivity increases and it is observed that the frequency ratio is varied in between 5.43 and 5.07. The experiment results and transmission line model proved that probe feed position almost have no effect on the frequency ratios and the operating frequencies.

CHAPTER 4

CALCULATION OF RESONANT FREQUENCY OF AN EQUILATERAL TRIANGULAR PATCH ANTENNA

There are two models defined in this thesis for calculating the resonant frequency of an equilateral triangular microstrip patch. One is based on dynamic permittivity, the other is based on effective permittivity expressions, and both are based on cavity model analysis.

4.1 Proposed Model 1

The geometry of the proposed model 1 is given as:

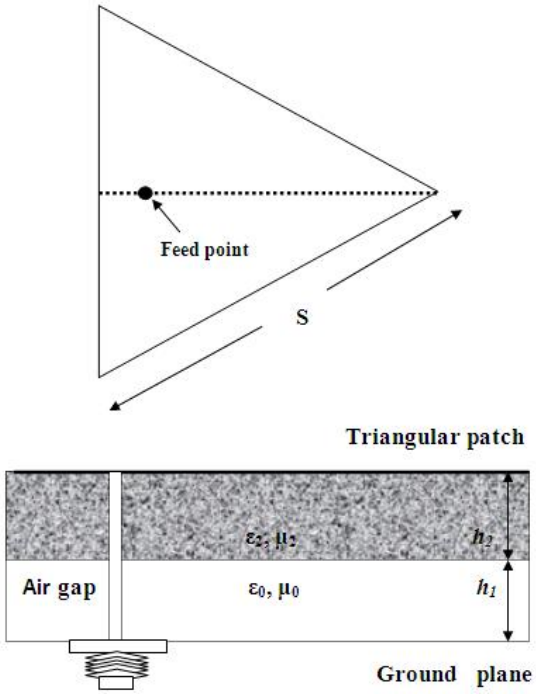

Figure 19: Tunable equilateral triangular microstrip antenna Model 1.

As mentioned in other studies there are various methods for finding resonant frequency. In this model, effective side-length, effective area, and dynamic permittivity are used to determine the resonant frequency. The analysis is done by cavity model and the steps are determined for calculating the resonant frequency of an equilateral triangular patch antenna.

$$h_{eq} = h + (\frac{h_1}{n^{1.2}}) \tag{67}$$

$h = h_1 + h_2$ is the total thickness of the equivalent model, n is the radial mode index value for nmth mode. In addition, the condition "$m + n + l = 0$" should be satisfied.

$$s_{eff} = \frac{2\pi a_{eff}}{3} \tag{68}$$

s_{eff} is defined as effective area of the triangular patch which counts the fringing field effects by using the effective side-length defined in [15] by using curve-fitting formula as:

$$a_{eff} = a\left\{1 + \left(\frac{2h}{\varepsilon_{r2} a\pi}\right) \ln\left(\frac{a}{Mnh + 3Mmh}\right) 1.41\varepsilon_{r2} + 1.77 + \frac{h}{a}(0.268\varepsilon_{r2} + 1.65)\right\}^{\frac{1}{2}} \tag{69}$$

where, *M* is the modal index coefficient which is obtained from the dynamic main capacitance expression of the circular patch [15].

The equivalent relative permittivity is defined by using cavity model is defined as:

$$\varepsilon_{req} = \frac{\varepsilon_{r2}(h_1 + h_2)}{(h_2 + \varepsilon_{r2} h_1)} \tag{70}$$

The dynamic capacitance is defined as; $C_{dyn}(\varepsilon_{req}, \varepsilon_{r0}) = C_{0,dyn}(\varepsilon_{req}, \varepsilon_{r0}) + C_{e,dyn}(\varepsilon_{req}, \varepsilon_{r0})$.The determination of the dynamic permittivity is done by using dynamic capacitance:

$$\varepsilon_{dyn} = \frac{C_{dyn}(\varepsilon_{r0}, \varepsilon_{req})}{C_{dyn}(\varepsilon_{r0} = \varepsilon_{req} = 1)} \tag{71}$$

Several formulations are derived for calculation of the static and main-field capacitance as in the rectangular patches. The formulations for dynamic main-field capacitance, static main capacitance are given and derivation is done by the eqns. 72-79:

$$c_{e,stat\,2} = \left(\frac{\varepsilon_0 \varepsilon_{reff}\, \pi a^2}{h}\right)\left(1 + \frac{2h}{\pi \varepsilon_{reff}\, a}\right)\ln\left(\frac{a}{Mnh + 3Mmh}\right) + 1.41\varepsilon_{r2} + 1.77 + \frac{h}{a}(0.268\varepsilon_{r2} + 1.65) \tag{72}$$

$$c_{e,dyn\,2} = \frac{c_{e,stat\,2}}{2}\,, c_{0,stat\,2} = \frac{\varepsilon_0 \varepsilon_{reff}\, \pi a^2}{h}, c_{0,dyn\,2} = 0.3525 c_{0,stat\,2} \tag{73}$$

and

$$c_{dyn\,2} = \frac{c_{0,dyn\,2}}{c_{e,dyn\,2}}$$

$$c_{e,stat\,1} = \left(\frac{\varepsilon_0 1 \pi a^2}{h}\right)\left(1 + \frac{2h}{\pi 1 a}\right)\ln\left(\frac{a}{Mnh + 3Mmh}\right) + 1.41\varepsilon_{r2} + 1.77 + \frac{h}{a}(0.268\varepsilon_{r2} + 1.65) \tag{74}$$

$$c_{e,dyn\,1} = \frac{c_{e,stat\,1}}{2} \tag{75}$$

$$c_{0,stat\,1} = \left(\frac{\varepsilon_0 1\pi a^2}{h}\right) \tag{76}$$

$$c_{0,dyn\,1} = 0.3525 c_{0,stat\,1} \tag{77}$$

$$c_{dyn\,2} = c_{0,dyn\,1} + c_{e,dyn\,1} \tag{78}$$

$$\varepsilon_{dyn} = \frac{c_{dyn\,2}}{c_{e,dyn\,1}} \tag{79}$$

By using ε_{dyn} eqn.79 and s_{eff} eqn.68 the resonant frequency formula is defined as:

$$f_{mnl} = \frac{2c}{3S_{eff}\left(\varepsilon_{dyn}\right)^{1/2}}\left(m^2 + mn + n^2\right)^{1/2} \tag{80}$$

Table 11: Resonant frequencies (MHz) for a=10cm, ε_{r2}=2.32, h_1 =0, h_2=1.59mm.

Mode	**Measured (MHz)**	**Proposed model 1**
TM_{10}	1280	1314
TM_{11}	2242	2299
TM_{20}	2550	2637
TM_{21}	3400	3492
TM_{30}	3824	3943
Error %		2.92

As seen in tables 11 and 12 the error that is obtained from the Model 1 is calculated for each mode and the average error is determined as 2.92 % and 1.5 %, respectively for the proposed antennas.

Table 12: Resonant frequencies (MHz) for a=8.7cm, ε_{r2}=2.32, h_1 =0, h_2=0.7mm.

Mode	**Measured (MHz)**	**Proposed model 1**
TM_{10}	1489	1510
TM_{11}	2596	2630
TM_{20}	2969	3025
TM_{21}	3968	4004
TM_{30}	4443	4529
Error %		1.50

Table 13: Comparison of resonant frequencies (in MHz) of an equilateral triangular microstrip antenna with air-gap for s=*15.5*mm, ε_2=*2.2* ε_0, h_2=*0.508*mm.

Mode	**h_1(μm)**	***f_r* measured**	**Proposed model 1**
TM_{10}	0	8324	8649
	280	9433	9834
	350	9512	9944
TM_{11}	0	14476	15211
	280	16667	17301
	350	16779	17479
Average error (%)			4.29

Two-layer geometry is also studied in the Model 1 and the resonant frequencies of the antennas for different thickness values are calculated and demonstrated in table 13. This evaluation is done for TM_{10} and TM_{11} modes and an average error of 4.29% error is obtained.

Table 14: Resonant frequencies (MHZ) s=100 mm, ε_2=10 for TM_{10} mode

h_2 (mm)	f_r Method of Moment	Proposed model 1
4	639	634
8	631	636
12	619	638
16	608	640

The comparison of the method of moment and Model 1 is done in table 14 for various thickness values and close conformity is obtained.

4.2 Proposed Model 2

A double-layered tunable equilateral triangular microstrip antenna is shown in Figure.20. The side-length of the equilateral triangular patch is *s*. The air-gap and substrate thicknesses are denoted as h_1 and h_2, respectively. The resonant frequency of the antenna can be determined from cavity model by using a proper equivalent model with effective structural parameters. For this purpose, various expressions for effective patch radius a_{eff} and effective relative permittivity ε_{eff} are defined in the literature for an equilateral triangular patch antenna [5]-[15].

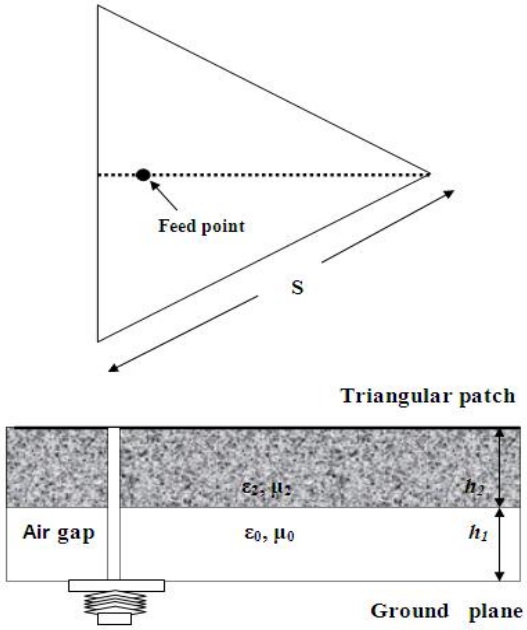

Figure 20: Tunable equilateral triangular microstrip antenna Model 2.

The equilateral triangular patch is replaced by an equivalent circular patch as in eqn.81.The radius of this circular patch is taken from [5] the form as:

$$a = \frac{3s}{2\pi} \tag{81}$$

A curve-fitting formula is widely used in order to obtain an effective patch radius [15]. An example of such formula has been given proposed in Aydın et al.

In this study, to propose an effective patch radius expression, their approach is modified for the equilateral microstrip antenna by considering modal effects:

$$a_{eff} = a\left\{1 + \left(\frac{2h}{\varepsilon_{r2} a\pi}\right) \ln\left(\frac{a}{Mnh + 3Mmh}\right) 1.41\varepsilon_{r2} + 1.77 + \frac{h}{a}(0.268\varepsilon_{r2} + 1.65)\right\}^{\frac{1}{2}} \tag{82}$$

Where h_t , h_1, h_2 , n, M are already determined in section 4.1.

The following effective permittivity for single-layered equivalent model taken from [15] will be used in our formulation as:

$$\varepsilon_{eff} = \frac{1}{2}(\varepsilon_{req} + 1) + \frac{1}{2}(\varepsilon_{req} - 1)(1 + \frac{12}{W/h_{eq}})^{-1/2} \quad (83)$$

Where, h_{eq} and W represent the effective height of the equivalent microstrip line and the width of the microstrip line, respectively. In order to provide the closest fit with those measures in the experimental study h_{eq} and W are approximated in the form:

$$h_{eq} = h_2 + (h_1/n^{1.2}) \quad (84)$$

$$W = 2\pi Ma(\frac{a}{a_{eff}})^{2.6} \quad (85)$$

The equivalent substrate permittivity ε_{req} expression is approximated with the help of cavity analysis as:

$$\varepsilon_{req} = \frac{\varepsilon_{r2}(h_1 + h_2)}{(h_2 + \varepsilon_{r2}h_1)} \quad (86)$$

Where h_1 and h_2 are thickness of the air-gap and substrate thickness, respectively. The total thickness is simplified with the formula $h_t = h_1 + h_2$ to generalize the two-layer structures as a single-layer structure. In the single-layer structure, h_1 is assumed zero. The effective patch of the equilateral triangular a_{eff} is replaced with a circular patch s_{eff} having an equivalent perimeter. The radius of this circular patch is taken in the following form as given in [15].

$$s_{eff} = \frac{2\pi a_{eff}}{3} \quad (87)$$

Then, the resonant frequency (f_r) of TM_{nm} modes of a single-layer equilateral

triangular microstrip-patch with and without air-gaps, f_r, is determined from the cavity model including the fringing fields at the open-end edge of the microstrip patch by using given eqns. 81-87:

$$f_r = \frac{2c\sqrt{m^2 + mn + n^2}}{3s_{eff}\sqrt{\varepsilon_{eff}}} \tag{88}$$

Where c is the velocity of light in free space, m and n denote the mode number; s_{eff} is the effective side-length of an equilateral triangular microstrip patch and ε_{eff} denotes the effective substrate relative permittivity.

The resonant frequencies of equilateral triangular antennas calculated with proposed method 2 introduced in this study and corresponding average percentage errors with and without air-gap are listed in tables. Beside experimental results, the most accurate methods are taken as reference to compare the calculated values.

The average percentage errors are calculated for an equilateral triangular antenna without air-gap for the method of moments (1.33) and most accurate method, $(f_r)_{GS}$, [14] in the literature (2.15) and for present model (0.44). A similar comparison is made for a high dielectric constant substrate.

The present formula, here is compared with other works [5]-[13] in the literature for high dielectric substrate permittivity ($\varepsilon_2 = 10\varepsilon_0$) and various substrate thicknesses (h_2=4 *to* 16*mm*) at TM_{10} mode. The results providing the best accuracy have been obtained by the theory of Garg and Long [5]-[12] using a new effective side-length expression for this case. The average percentage of error of in theory by Garg and Long [12] is around 1.5. In this study, nevertheless, and using a combination of the new effective patch radius and effective permittivity expressions, this average is reduced to 1.31 for various substrate thicknesses (h_2=4 *to* 16*mm*).

The resonant frequencies of a tunable equilateral triangular microstrip antenna with variable air-gap in between the substrate and the ground plane are compared with the only available measurement results in the literature and another accurate cavity model analysis. The average percentage errors in this case are 0.69 for the previous model, and 0.46 for present model.

Table 15: Comparison of resonant frequencies (in MHz) of an equilateral triangular microstrip antenna without air-gap.

	Mode	f_r measured	Method of Moment		results [5]		proposed model 2		ht/λ
			$(f_r)_{MOM}$	error (%)	$(f_r)_{GS}$	error (%)	(f_r) Eqn. 8	error (%)	
s=100mm ε_2=2.32 ε_0 h_2=1.59mm	TM_{10}	1280	1288	0.63	1285	0.39	1275	0.39	0.0068
	TM_{11}	2242	2259	0.76	2226	0.71	2221	0.94	0.0119
	TM_{20}	2550	2610	2.35	2570	0.78	2549	0.04	0.0135
	TM_{21}	3400	3454	1.59	3400	0.00	3401	0.03	0.0180
	TM_{30}	3824	3875	1.33	3485	8.87	3854	0.78	0.0203
	Average error (%)		1.33		2.15		0.44		

Table 16: Comparison of resonant frequencies (MHz) of an equilateral triangular microstrip antenna with air-gap for s=15.5mm, ε_2=2.2 ε_0, h_2=0.508mm.

Mode	h_1(μm)	f_r measured	[5] results		proposed model 2		ht/λ
			$(f_r)_{GS}$	*Error (%)*	(f_r)	*Error (%)*	
TM_{10}	0	8324	8325	0.01	8224	1.20	0.0141
	280	9433	9447	0.15	9423	0.11	0.0248
	350	9512	9547	0.37	9546	0.36	0.0272
TM_{11}	0	14476	14420	0.39	14408	0.47	0.0161
	280	16667	16363	1.82	16591	0.46	0.0438
	350	16779	16535	1.45	16805	0.15	0.0480
Average error (%)			0.70		0.46		

It can concluded that the average percentage of error values calculated as in tables below for with and without air-gap cases indicate the efficiency of the proposed formulation over the most accurate methods presented in the literature. Proposed model 2, accounts, the fringing fields accurately when the substrate is given by *h/λ* from 0.0068 to 0.048. Excellent agreement is revealed except for just one case with and without air-gap case. Nevertheless, it is observed that generally it exhibits

smaller error ratios than the most accurate and recent methods in the literature.

Table 17: Resonant frequencies (MHZ) for s=100mm, $\varepsilon_2 = 10\varepsilon_0$ TM_{10} mode

h_2 (mm)	f_r Method of Moment	Results [5]		Proposed model 2		ht/λ
		fr	Error (%)	fr	Error (%)	
4	639	623	2,503	628	1,721	0.0088
8	631	616	2,377	622	1,426	0.0168
12	619	612	1,130	612	1,130	0.0248
16	608	608	0	602	0,986	0.0324
Average error (%)		1,502		1,316		

4.3 Comparison of proposed model 1, model 2 and simulated results (CST)

An antenna with a side-length of 10cm, permittivity value of 2.32, and a thickness value of 1.59mm is considered and the proposed Model 1 and the Model 2 are compared with the experimental and CST simulation results for various modes. The CST results achieved an average error of 0.97 % while the Model 1 and the Model 2 achieved an average error of 2.9% and 0.44%, respectively.

The better accuracy is obtained with Model 2. The error, which is obtained from TM_{10}, TM_{11}, TM_{20}, $TM_{21,}$ and TM_{30} is 0.39%, 0.93%, 0.03%, 0.02% and 0.7%, respectively. The HFSS results achieved 2210 MHz for TM_{11} mode. A similar 3D-geometry of the antenna is given in appendix.

Table 18: Resonant frequencies (MHz) calculated with proposed model 1, 2 and simulated results for a=10cm, ε_{r2}=2.32, h_1 =0, h_2=1.59mm.

Mode	Measured (MHz)	Proposed model 1	Proposed model 2	CST Results
TM_{10}	1280	1314	1275	1268
TM_{11}	2242	2299	2221	2202
TM_{20}	2550	2637	2549	2539
TM_{21}	3400	3492	3401	3371
TM_{30}	3824	3943	3854	3807
Error %		2.9	0.44	0.97

Later, another antenna is investigated which has a side-length of 8.7cm and a thickness value 0.78cm with the same permittivity value of the previous antenna. The resonant frequencies of the afore-mentioned antenna are given with the table below. The Model 1, Model 2, and the CST achieved an average error of 1.5%, 0.07% and 0.82%, respectively.

The Model 2 is once again achieved better accuracy than the other model and the CST. The error, which is obtained from TM_{10}, TM_{11}, TM_{20}, $TM_{21,}$ and TM_{30} is 0.03%, 0.03%, 0.02%, 0.05 and 0.04%, respectively. The mentioned antenna is also designed in HFSS and for TM_{11} mode 2540 MHz resonant frequency is obtained with a return loss -28.57dB. The resonant frequency of the designed antenna yields close conformity. The assignment of the boundaries and the reflection coefficient-frequency graph is given in appendix as an example.

Table 19: Resonant frequencies (MHz) calculated with proposed model 1, 2 and simulated results for a=8.7cm, ε_{r2}=2.32, h_1 =0, h_2=0.78cm.

Mode	Measured (MHz)	Proposed model 1	Proposed model 2	CST Results
TM_{10}	1489	1510	1484	1476
TM_{11}	2596	2630	2588	2572
TM_{20}	2969	3025	2976	2952
TM_{21}	3968	4004	3945	3928
TM_{30}	4443	4529	4461	4412
Error %		1.5	0.07	0.82

The antenna with a side-length of 41cm, permittivity value of 10.5, and a thickness value of 0.7cm is considered and the resonant frequencies are determined with models presented and CST. The results showed that for high dielectric substrates the model 1 and 2 achieved satisfactory agreement when compared to the experimental results with an average error of 1.17% and 0.84%, respectively while the CST had an average error of 0.84%. A design of this antenna with a side-length is done by using HFSS and for the TM11 mode 2453 MHz resonant frequency is obtained with a return loss of -20.9 dB.

Table 20 : Resonant frequencies (MHz) calculated with proposed model 1, 2 and simulated results for a=41mm, ε_{r2}=10.5, h_1 =0, h_2=0.7cm.

Mode	Measured (MHz)	Proposed model 1	Proposed model 2	CST Results
TM_{10}	1519	1678	1502	1496
TM_{11}	2637	2942	2644	2612
TM_{20}	2995	3363	3019	2992
TM_{21}	3973	4435	3997	4024
TM_{30}	4439	4996	4500	4424
Error %		1.17	0.63	0.84

CHAPTER 5

SHORTING PIN-LOADED DUAL-FREQUENCY ANTENNAS

As mentioned in introduction section, the demand on the dual frequency applications increased the attention on microstrip antennas. Slot-loaded, slit-loaded antennas are designed to provide dual frequency antennas. Shorting pin-loaded antennas are commonly preferred among those due to their advantages. The distance between the shorting pin and the feed is measured in terms of millimeters so the distances are so close to each other that it may cause some manufacturing problems. Achieving higher frequency ratio is one of the most important aims in designing dual frequency antennas. Various applications like satellite positioning systems and SAR systems require high frequency ratios. Although shorting pin-loaded, microstrip antennas have some manufacturing difficulty they are popular in such systems since they provide high frequency ratios.

The studies presented in literature showed the frequency ratio, permittivity, feed position and shorting pin position effects experimentally. Although there is a transmission line model on computation of the resonant frequencies of a shorting pin-loaded equilateral triangular patch, this study presents more accurate model, which is based on cavity model analysis.

The model will be determined and discussed in the following sections. The geometry of a shorting pin-loaded triangular patch will be demonstrated; the results and comparisons will be presented in 5.1.

5.1 Computation of Operating Frequencies of a Shorting Pin-Loaded Equilateral Triangular Patch Antenna

5.1.1 Determination of Operating Frequencies of Shorting Pin-Loaded ETMP

The geometry of a shorting pin-loaded dual-frequency equilateral triangular patch antenna is given in figure 21.

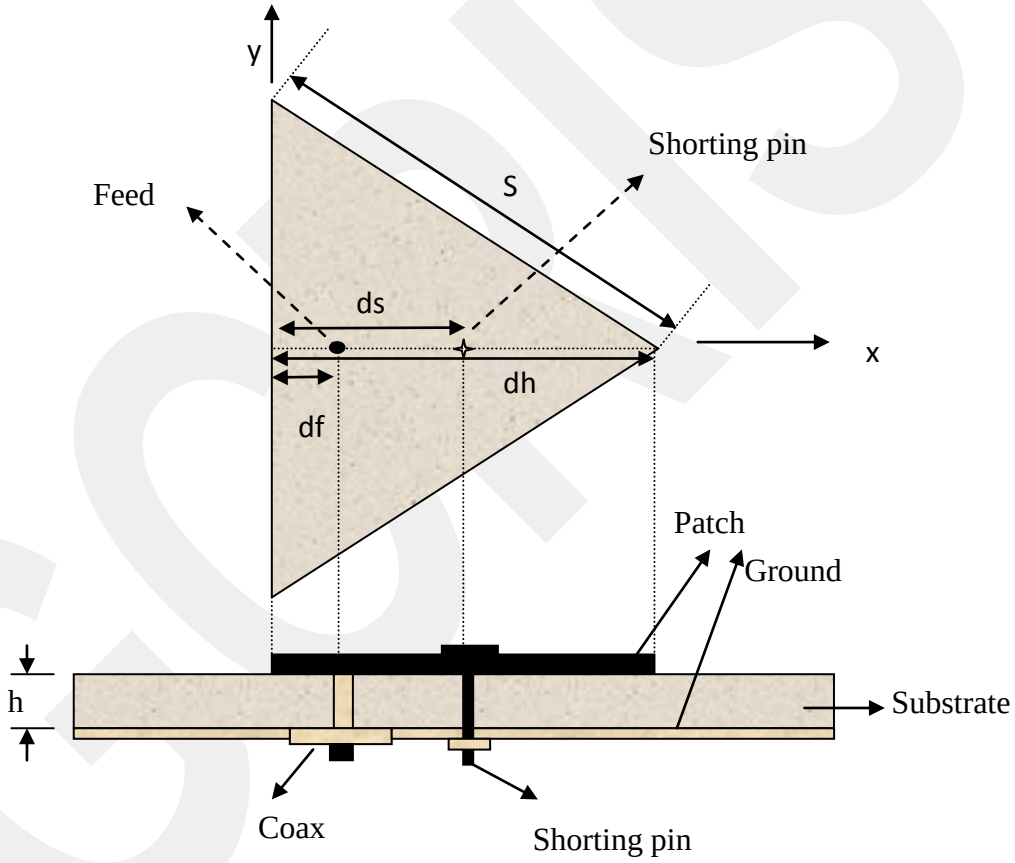

Figure 21: Geometry of a shorting pin-loaded equilateral triangular patch antenna.

The thickness of the substrate and the side-length of the equilateral triangular patch are represented as *h* and *S* respectively. The distance from the side of triangular to the shorting pin is denoted as *ds* , the distance between the side-length and the probe feed is *df* and the distance between side-length to the tip of the triangle is *dh*. The effective side-length and effective permittivity are defined in various ways in

literature [15]. Since dual-band microstrip antennas have one upper and one lower frequency, two different formulations are developed to express resonant frequencies of a dual-band a shorting pin-loaded equilateral triangular patch antenna. In various application and experiments in the literature, it is mentioned that feed probe position has no effect on the upper and lower frequency of the antenna [44]. Since the resonant frequencies are almost constant with the probe position variation, the probe position *(df)* has been ignored in theoretical calculations.

The cavity model depends on the assumption of perfect magnetic-wall, which is used to determine the operating frequencies. The resonant frequency is defined as:

$$f_r = \frac{2c}{3S_{eff}\left(\varepsilon_{eff}\right)^{1/2}}(m^2 + mn + n^2)^{1/2} \tag{89}$$

n and m are the radial mode index values for nmth mode, m, n, l are integers that cannot be zero simultaneously and eqn.90 should be satisfied :

$$m + n + l = 0 \tag{90}$$

An equivalent circular patch replaces the shorting pin-loaded equilateral triangular patch and the radius of this circular patch is taken from the form as in [15]:

$$s_{eff} = \frac{2\pi a_{eff}}{3} \tag{91}$$

A curve-fitting formula is widely used in order to obtain an effective patch radius [15]. The effective patch radius is proposed by Aydın et.al [15] as in eqn.92:

$$a_{eff} = a\left\{1 + \left(\frac{2h}{\varepsilon_{r2}a\pi}\right)\ln\left(\frac{a}{Mnh + 3Mmh}\right)1.41\varepsilon_{r2} + 1.77 + \frac{h}{a}(0.268\varepsilon_{r2} + 1.65)\right\}^{\frac{1}{2}} \tag{92}$$

$_M$ is the modal index coefficient, which is obtained from the dynamic main

capacitance expression of the circular patch.

As in presented in literature the modal indexes and constants are given in [49] as:

$$\begin{aligned} &TM_{10},\ M = 0.3525,\ for\ n = 1,\ m = 0 \\ &TM_{11},\ M = 0.1841,\ for\ n = 1,\ m = 1 \\ &TM_{20},\ M = 0.2856,\ for\ n = 2,\ m = 0 \\ &TM_{21},\ M = 0.3054,\ for\ n = 2,\ m = 1, \\ &TM_{31},\ M = 0.4201,\ for\ n = 3,\ m = 1 \end{aligned} \tag{93}$$

The following effective permittivity for single-layered equivalent model taken from [15] will be used in the proposed formulation as:

$$\varepsilon_{eff} = \frac{1}{2}(\varepsilon_{r2} + 1) + \frac{1}{2}(\varepsilon_{r2} - 1)(1 + \frac{12}{W/h_{eq}})^{-1/2} \tag{94}$$

Where, h_{eq} and W represent the effective height of the equivalent microstrip line and its width, respectively. In order to provide the closest fit, h_{eq} and W are approximated in the eqns.95 and 96:

$$W = 2\pi Ma(\frac{a}{a_{eff}})^{2.6} \tag{95}$$

$$h_{eq} = (h/n^{1.2}) \tag{96}$$

A ratio (u) is defined between the shorting pin position and the distance between tip of the triangle patch to the side-length of the triangle patch, which is determined as:

$$u = \frac{ds}{dh} \tag{97}$$

For calculating the upper resonant frequency, a correction factor CF_{upper} is defined by using curve-fitting tools of MATLAB, to add the shorting pin position effect to the upper resonant frequency as:

$$CF_{upper} = \frac{(-5.305u^3) + (8.597u^2) + (-2.937u) + 2.035}{1.88} \quad (98)$$

Therefore, the upper resonant frequency that varies with the variation of the pin position is defined as:

$$f_{r,upper} = f_r CF_{upper} \quad (99)$$

All the experiments show that the lower resonant frequency is affected from the pin position and permittivity values of the substrates. To incorporate the effects of pin position and permittivity a correction factor defined for lower frequency as CF_{lower} . The correction factor of pin position effect and permittivity effect is found by using MATLAB curve-fitting tools and is formulized as:

$$CF_{lower} = (2e^{-2.624u} + 0.7351e^{1.981u} + (4.4 - \varepsilon_{r2})0.04^{0.654})^{-1} \quad (100)$$

$f_{r,lower}$ of a shorting pin-loaded equilateral triangular microstrip patch, which is affiliated to pin position and permittivity of the substrate is determined by the cavity model including the fringing fields as:

$$f_{r,lower} = f_r CF_{Lower} \quad (101)$$

As mentioned in introduction part, one of the most important parameter in dual-frequency operation is the frequency ratio, which is expressed as:

$$frequency\ ratio = \frac{f_{r,upper}}{f_{r,lower}} \quad (102)$$

5.2.1 Results and Discussion

The resonant frequencies of a shorting pin-loaded triangular patch antenna are calculated by curve fitting and empirical formulas. Frequency ratio is also

investigated in this section. The relations between shorting pin positions and frequency ratios are determined and compared with the experimental and theoretical results obtained in the literature. The graphs of comparison of the results of the present study and experimental study presented.

All the experimental studies showed that the null voltage point of an equilateral triangular patch occurs at a ratio *u=0.33.* The study presented here is also agreed that the null voltage point occurs in *u=0.33.*The smaller upper frequency and the larger lower frequency observed at this position so the smallest frequency ratio is in the null voltage point. The frequency ratio and shorting pin position ratio of the presented in figure 22 agrees the experimental results well.

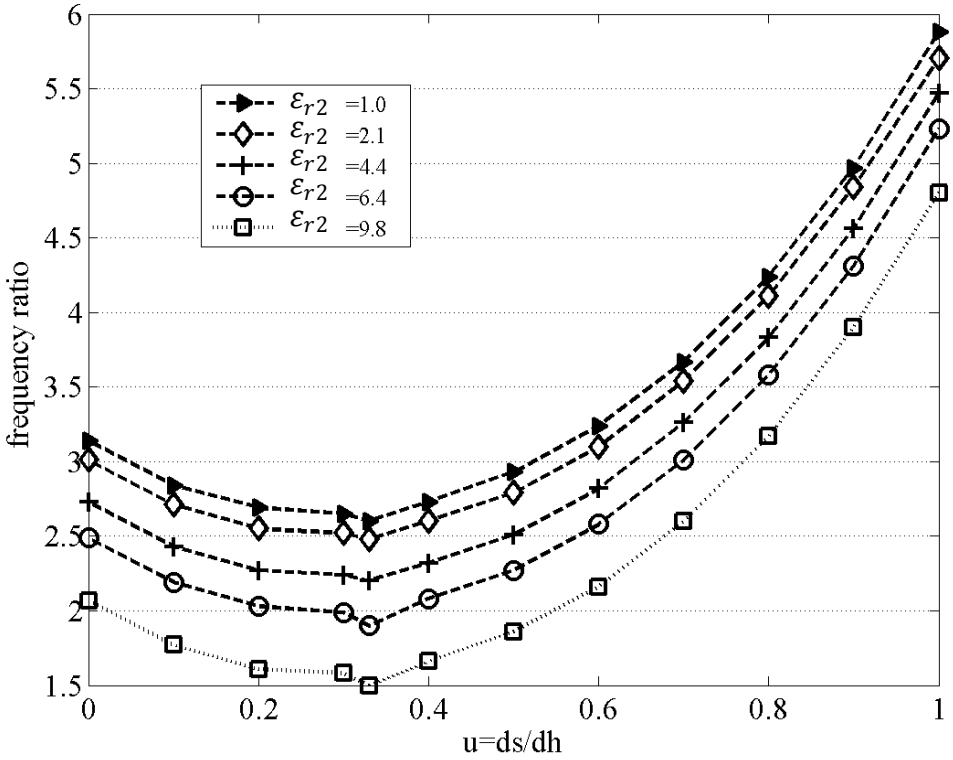

Figure 22: Frequency ratio values with respect to *u* for different permittivity values.

The minimum frequency ratio varied in between 1.68 and 2.81 in [45] and it is varied from 1.57 to 2.71 in the presented study. It is observed that the frequency ratio increase if the permittivity value and the distance from null voltage point (*u=0.33*) increases as in [45].Maximum frequency ratio observed at the tip of the triangle

which means the u=1 and varied from5.43 to 5.07 in experimental results. It is also deduced from the graphs that the increase in permittivity cause a decrease in frequency ratio value in any particular pin position value.

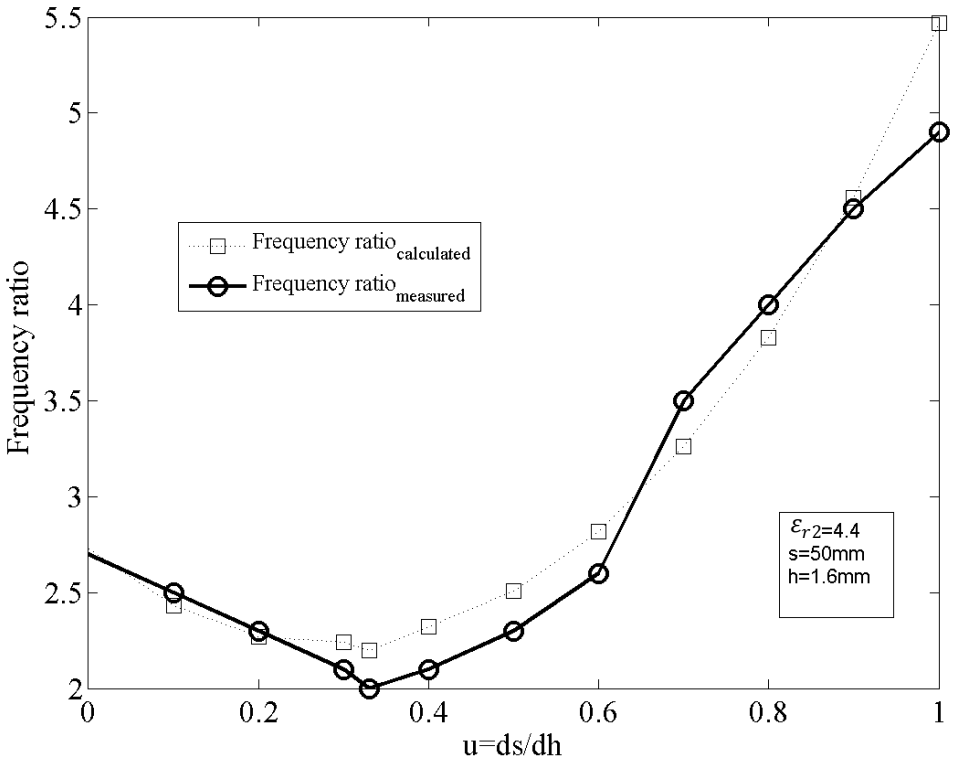

Figure 23: The frequency ratio comparison of present method and experimental results of an antenna with ε_{r2}=4.4, h=1.6mm, s=50mm.

The lowest frequency ratio occurred at null voltage point (u=0.33) as seen in figure 23. The effects of null voltage point on both upper and lower frequency can be observed in figure 24. The comparison of the experimental, transmission line analysis and the present study are given in the figure 24.

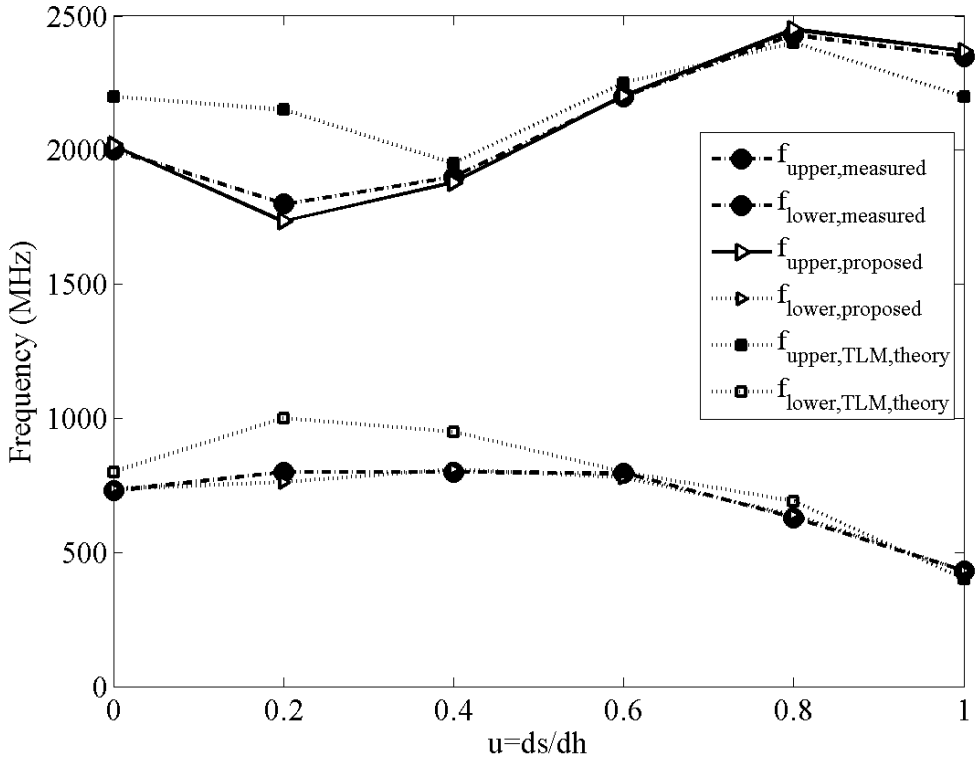

Figure 24: Comparison of experiment, transmission line model and the presented study results for ε_{r2}=4.4, h=1.6mm, s=50mm.

The figure above shows us that a good agreement is obtained compared to the experimental results and has much accuracy than the transmission line model calculation.

The resonant frequencies of several antennas which are presented in literature in [42], [45] and [46] respectively, compared and error calculations are given in table below; The theory of the upper and lower frequencies of the presented study are examined and compared with the measured values for different permittivity, thickness, side-length and pin position values

Table 21: Comparison of three antennas, operating frequencies and error

Antenna type	ε_{r2}	s (mm)	u (ds/dh)	h (mm)	$f_{r,upper}$ meas MHz	$f_{r,lower}$ meas MHz	$f_{r,upper}$ Proposed MHz	$f_{r,lower}$ Proposed MHz	Error % $f_{r,upper}$	Error % $f_{r,lower}$
1	4.4	50	0.991	1.6	2276	464	2384	442	4.74	4.74
2	4.4	50	0.33	0.762	1886	766	1815	805	3.76	5.09
3	3.0	59.9	0.255	0.762	1900	750	1770	733	6.84	2.26

The comparison of three antennas is given in table. The theory of the upper and lower frequencies of the presented study examined and compared with the measured values for different permittivity, thickness, side-length and pin position values. Error calculation is done for each antenna for both upper and lower frequencies. The upper frequency error is varied in between 3.76%-6.84% for three antennas and the lower frequency error was in between 2.26%-5.09%. The average error is obtained for upper frequency is 5.11% while the average error for lower frequency is 4.3%.

CHAPTER 6

CONCLUSION

The study presented in this thesis consists of two main stages. The purpose of first stage is to determine the resonant frequency of an equilateral triangular patch antenna. In the second stage, calculations are carried out to find the operational frequencies of a shorting pin-loaded dual-frequency equilateral triangular patch antenna.

In the first stage, and upon completing the literature review, a modified expression is derived for the computation of resonant frequency of an equilateral triangular patch antenna. For this purpose, an equilateral triangular patch that is fed by coax-probe is considered and the cavity model analysis is used for calculating the resonant frequency. The cavity model has been selected since it requires less time for computation and has a simple structure. At this stage, two models are proposed for computation.

In the first model, the dynamic permittivity expression is used to find the resonant frequency and in the second model - by replacing the dynamic permittivity value with the effective permittivity – agreement that is more satisfactory is obtained when compared to the experimental values presented in the literature. In order to insert the fringe field-effects, an effective side-length expression is derived. Then, that triangular patch is defined as a circular patch. The perimeter of the equilateral triangular becomes equal to a circular patch, which is used to determine the effective side-length. The effective area is derived by means of this expression. For both models, two thickness values are defined for the substrate and the air-gap in the antenna structure.

Using the dynamic permittivity expression to compute the resonant frequency, Model 1 is tested for several antennas presented in the literature. The results are compared with the measured values for different modes. An average of 2.92% and 1.5% error is detected for different side-length and thickness values of single-layer geometry. The formulation is extended to two-layer geometry, and the outcomes are compared with other experimental results, from which an average 4.29% error is obtained. The resonant frequencies of an antenna with a side-length of 100mm and permittivity value of 10 are determined for the TM_{10} mode, and then compared with the method of moment, yielding close conformity.

Model 2, using the effective permittivity expression, is extended to a two-layer structure by changing the thickness parameter of the air-gap. This structure is turned into a single-layer structure by reducing the air-gap thickness to zero. Then, the formulation is tested for different thicknesses and permittivity values. In this calculation, the thickness of the air-gap is altered and the two-layer structure is also studied. The results are compared with the ones from moment method yielding an average error of 1.33%, and with a cavity model solution presented in [6] yielding an average 2.15% error. These outcomes indicate that, Model 2 has achieved a satisfactory agreement when compared to the other results in the literature. At a later stage, the formulation tested for different thicknesses and side-length values, subsequently compared with experimental results. An average 0.46% error is obtained for single-layer and 1.316% for two-layer geometry as well.

The proposed models are compared with the CST results. Model 1 achieved an average 2.9% error, while Model 2 provided a far better accuracy of 0.44% average error – a percentage that is lower when compared to the CST results at 0.97%. These two models are also tested for two other single-layer antennas, with different side-length, permittivity, and thickness values. The proposed Model 2 had an average error between 0.07%-0.63% which is, once again, more accurate than CST sample at 0.82%-0.84% error.

In the second stage of the study, a shorting pin-loaded, dual-frequency, antenna is analyzed upon completing the literature pertaining to the dual-frequency microstrip antennas. The related studies in the literature suggest inserting a shorting pin to a

microstrip patch is a preferable way of forming dual frequency operation because of its simple structure and smaller size. This study is conducted, as such, as a result of the advantages of the shorting pin-loaded equilateral triangular patch antenna. The operation frequencies of these antennas are calculated using the method proposed in this thesis and is based on cavity model. Effective side-length and effective permittivity expressions are used to analyze the resonant frequency. To incorporate the permittivity and the shorting pin effects, two different correction factors are determined to compute the upper and lower resonant frequency values. Later, these results are compared with the ones available in the literature, and, as far as the author and the literature reveals are concerned, the model is the first that calculates the operating frequencies of a shorting-pin loaded triangular microstrip patch antenna using the cavity model.

In short, different frequency ratio ($f_{r,upper}/f_{r,lower}$) results are obtained for different side-length, permittivity, thickness, and shorting pin position values. A null voltage point is determined depending on the shorting pin position. The results indicate that a minimum frequency ratio is obtained at the null voltage point ($u=0.33$). The maximum lower frequency and the minimum upper frequency are also obtained at the afore-mentioned point. The minimum frequency ratio decreases if the permittivity of the substrate increases. The frequency ratio increases with an increase in the distance of the shorting pin position from the null voltage point. The maximum frequency ratio is obtained at the tip of the triangular patch.

On the other hand, the studies that are presented in the literature reveal that, the probe feed position does not affect the upper and lower frequencies. The results presented in this study conform to those obtained from the experimental and transmission line models as per the literature [45]. A change in probe feed position also changes the upper and lower frequency to an insignificant amount; thereby excluding it from the model is proposed in this study.

In conclusion, the study presented in section 5.1 achieved satisfactory agreement with the experimental results. The average error obtained from this study varied in between 3.79% to 6.84% for several antennas subjected in literature. It has been observed that these results are the closest to those in the literature, and that they have

a better accuracy than the transmission line model results. The variation of the frequency ratio according to the changes in permittivity, shorting pin position and thickness parameters also have been stated with graphs in section 5.2.1

Several experiments in the literature have revealed that inserting multiple shorting pins to a triangular patch modifies the impedance and bandwidth. Single shorting pin tends to provide a narrower bandwidth when compared to the multiple versions. Based on this outcome, computation of the operational frequencies of a multiple shorting pin-loaded microstrip antenna can be a future work.

REFRENCES

[1]. Deschamps, G. A., "Microstrip Microwave Antennas", *Proc.3rd USAF Symposium of Antennas,* 1953

[2]. Munson, R. E., "Single Slot Cavity Antennas Assembly," *U.S. Patent* no.3713162, Jan 23, 1973

[3]. Munson. R. E., "Conformal Microstrip Antennas and Microstrip Phased Arrays," *IEEE Trans. Antennas Propagation,* Vol.AP-22, pp.74-78, Jan 1974

[4]. Howell, J. Q., "Microstrip Antennas," *IEEE Trans. Antennas Propagation,* Vol.Ap-23, pp.90-93, Jan 1975.

[5]. Guha, D. and J. Y. Siddiqui, "Resonant Frequency of Equilateral Triangular Microstrip Antenna with and without Air-gap," *IEEE Trans. Antennas and Propag.,* Vol. 52, No. 8, pp.2174-2177, August 2004.

[6]. Gürel, Ç. S. and E. Yazgan, "New Computation of the Resonant Frequency of a Tunable Equilateral Triangular Microstrip Patch," *IEEE Transactions on Microwave Theory and Techniques,* Vol. 48, No.3, pp.334-338, March 2000.

[7]. Gang, X., "On the Resonant Frequencies of Microstrip Antennas," *IEEE Trans. Antennas and Propag.,* Vol. 37, No. 2, pp. 245-247, Feb. 1989.

[8]. Güney, K., "Resonant Frequency of a Triangular Microstrip Antenna," *Microwave Opt. Technol. Lett*., Vol.6, pp.555-557, July 1993.

[9]. Kumprarsert, N. and K.W.Kiranon, "Simple and Accurate for the Resonant Frequency of the Equilateral Triangular Microstrip Patch Antenna," *IEEE Trans. Antennas and Propag.*, Vol. 42, No.8, pp.1178-1179, Aug.1994.

[10]. Dahele, J.S. and K.F.Lee, "On the Resonant Frequencies of the Triangular Patch Antenna," *IEEE Trans. Antennas and Propag.*, vol. AP-35, No.1, pp.100-101, Jan 1987.

[11]. Helszajn, J. and D. S. James, "Planar Triangular Resonators with Magnetic Walls," *IEEE Trans. Microwave Theory Tech.*, Vol. MTT-26, No.2, pp. 95–100, Feb. 1978.

[12]. Garg, R. and S. A. Long, "An Improved Formula for the Resonant Frequency of the Triangular Microstrip Patch Antenna," *IEEE Trans. Antennas Propagat.*, Vol. AP-36, No.4, pp. 570-573, Apr. 1988.

[13]. Chen, W., K. F. Lee, and J. S. Dahele, "Theoretical and experimental studies of the resonant frequencies of equilateral triangular microstrip antenna," *IEEE Trans. Antennas Propagat.*, Vol. 40, No.10, pp. 1253–1256, Oct. 1992.

[14]. Gürel, Ç. S., E. Aydın, and E. Yazgan, "Computation and optimization of resonant frequency and input impedance of a coax-fed circular microstrip antenna," *Microwave and Optical Technology Letters*, Vol. 49, No. 9, pp.2263-2267, Sept. 2007.

[15]. Aydın, E. and S.Can, "Modified resonant frequency computation for tunable equilateral triangular microstrip patch," *IEICE Electronics Express*, Vol. 7, No.7, pp.500-505, 2010.

[16]. Stutzman, W.L. and Thiele, G.A., Antenna Theory and Design, John Wiley & Sons, Inc,1998.

[17]. Balanis, C.A., Antenna Theory: Analysis and Design, John Wiley & Sons, Inc, 1997.

[18]. Garg, R., Bhartia, P., Bahl, I., Ittipiboon, A., Microstrip Antenna Design Handbook, Artech House, Inc, 2001.

[19]. Richards, W.F., Microstrip Antennas, Chapter 10 in Antenna Handbook: Theory Applications and Design (Y.T. Lo and S.W. Lee, eds.), Van Nostrand Reinhold Co., NewYork, 1988.

[20]. Nakar, P. S., Thesis *Master of Science* "Design of a compact Microstrip Patch Antenna for use in Wireless/Cellular Devices."

[21]. James, J.R. and P.S.Hal1, "Handbook of Microstrip Antennas", Peter Peregrinus Ltd., IEE, 1989

[22]. Karaboğa, D., K. Guney, N. Karaboğa, and A. Kaplan, "Simple and accurate effective side expression obtained by using a modified genetic algorithm for the resonant frequency of an equilateral triangular microstrip antenna," *Int. J. Electron.*, Vol. 83, pp. 99–108, Jan. 1997.

[23]. Dahele, J. S. and K. F. Lee, "On the resonant frequencies of the triangular patch antenna," *IEEE Trans. Antennas Propagat.*, Vol. AP-35, No.1, pp. 100–101, Jan. 1987

[24]. Chew, W. C. and J. A. Kong, "Effects of fringing field on the capacitance of circular microstrip disk," *IEEE Trans. Microwave Theory Tech.*, Vol. MTT-28, No.2, pp. 98–104, Feb. 1980.

[25]. Verma, A. K. and Z. Rostamy, "Resonant frequency of uncovered and covered rectangular microstrip patch using modified Wolff model," *IEEE Trans. Microwave Theory Tech.*, Vol. MTT-41, No.1, pp. 109–116, Jan. 1980.

[26]. Guha, D. "Resonant frequency of circular microstrip antennas with and without air-gaps," *IEEE Trans. Antennas Propagat.*, Vol. 49, No.1, pp. 55–59,Jan. 2001.

[27]. Suzuki, Y. and T. Chiba, "Computer analysis method for arbitrarily shaped microstrip antenna with multi-terminals," *IEEE Trans. Antennas Propagat.,* Vol. AP-32, No.6, pp. 585-590, June 1984

[28]. Singh, R., A. De, Garg, R., and R. S. Yadava, "Comments on an improved formula for the resonant frequency of the triangular microstrip patch antenna," *IEEE Trans. Antennas Propagat.,* Vol. 39, No.9, pp. 1443-1445, Sept. 1991.

[29]. Güney, K., "Comments on 'on the resonant frequencies of the microstrip antennas," *IEEE Trans. Antennas Propagat.*, Vol. 42, No.9, pp.1363-1365, Sept. 1994.

[30]. Bahl, I. J. and P. Bhartia., "Radiation characteristics of a triangular microstrip antenna," *Natural Sciences and Engineering Research Council of Canada*, Vol. 35, pp. 214-219, May 1981.

[31]. Nasimuddin,K. E. and A.K. Verma, "Resonant frequency of an equilateral triangular microstrip antenna" *Microwave and Optical Technology Letters*, Vol. 47, No. 5, pp.485-489, December 2005.

[32]. *Gao, S. and J. Li*, "FDTD analysis of a size-reduced, dual-frequency patch antenna," *Progress In Electromagnetics Research*, Vol. 23, 59-77, 1999

[33]. Aydın, E. “Computation of a Tunable Slot-Loaded Equilateral Triangular Microstrip Antenna” Journal *of Electromagnetic Waves and Applications*, Vol. 23, No. 14/15, pp. 2001-2009, 2009

[34]. Bhatnagar, P. S., J. P. Daniel, K. Mahdjoubi, and C. Terret, “Experimental study on stacked triangular microstrip antennas,” *Electron. Lett*, Vol. 22, No.16, pp. 864- 865, July 1986.

[35]. Wong, K. L. and W. S. Chen, “Compact microstrip antenna with dual frequency operation,” *Electron Lett*., Vol. 33, No.8, pp. 646-647, Apr. 1997.

[36]. Lu, H. and K.. L. Wong, “Single-feed dual-frequency equilateral-triangular microstrip antenna with pair of spur lines,” *Electron Lett*., Vol. 34, No.12, pp. 1171-1173, Jun. 1998.

[37]. Wong, K.L., S. T. Fang and J.H. Lu, “Dual frequency equilateral triangular microstrip antenna with a slit,” *Microwave Optical Technol. Lett*., Vol. 19, No.5, pp. 348-350, Dec. 1998.

[38]. Wong, K.L., M.C. Pan, and W.H. Hsu, “Single feed dual frequency triangular microstrip antenna with a V shaped slot,” *Microwave Optical Technol. Lett.*, Vol. 20, No.2, pp. 133-134, Jan. 1999.

[39]. Fang, S. T., and K.L Wong, “A dual frequency equilateral-triangular microstrip antenna with a pair of narrow slots,” *Microwave Optical Technol. Lett.*, Vol. 23, No.2, pp. 82-84, Oct. 1999.

[40]. Lu, J-H., C-L. Tang, and K. L. Wong, “Novel dual frequency and broadband designs of slot-loaded equilateral triangular microstrip antennas,” *IEEE Trans. Antennas Propagat*., Vol. 48, No.7, pp.1048-1054, July 2000.

[41]. Pan, S.C. and K. L. Wong, “Design of Dual-frequency microstrip

antennas with a shorting pin loading" *Antennas and Propagation Society International Symposium*, Vol.1, pp.312 -315, 21-26 Jun. 1998.

[42]. Pan, S. C and K.L. Wong, "Dual frequency triangular microstrip antenna with a shorting pin," *IEEE Trans. Antennas Propagat.*, Vol. 45, No.12, pp. 1889–1891, Dec. 1997.

[43]. Mythili, P., and A. Das "Comments on simple and accurate formula for the resonance frequency of the equilateral triangular microstrip patch antenna" *IEEE Trans. Antennas Propogation*, Vol.48 No.1. pp.636, Jan. 2000.

[44]. Wong, K.L. and S. C. Pan, "Compact triangular microstrip antenna" *Electron Lett.*, Vol. 33, No.6, pp. 433-434, Mar. 1997.

[45]. Pant, R.,P. Kala, R. C. Saraswat and S. S. Pattnaik, "Analysis of dual frequency equilateral triangular microstrip patch antenna with shorting pin" *Microwave Optical Technol. Lett*., Vol.3, No.2, pp.62-68, Apr. 2008.

[46]. Shang, F. and Ying-Zeng Y., "Analysis and Design of the Circular-Disk Antenna with a Shorting Pin", *IEEE Antennas and Propagation Magzaine,*Vol.52, No.2, pp.96-98, April 2010.

[47]. Luan,X.Z, Fang Shao-Jun and Tan Ke-jun, "Analysis and Optimization Design of Compact Microstrip Patch Antennas Loaded with Shorting Pins" *IEEE International Workshop on Antenna Technology*, pp.529, Mar.2005.

[48]. Ansari,J. A, P. Sing and N. P. Yadav, "Analysis of shorting pin-loaded half disk patch antenna for wideband operation", *Progress In Electromagnetics Research C*, Vol.6, pp.179-192, 2009

[49]. Wollf, I. and N. Knoppik, "Rectangular and Circular Microstrip Disk Capacitors and Resonators" *IEEE Transactions on Microwave Theory and Techniques*, Vol. MTT-22, No. 10, pp.857-864, Oct.1974.

APPENDIX

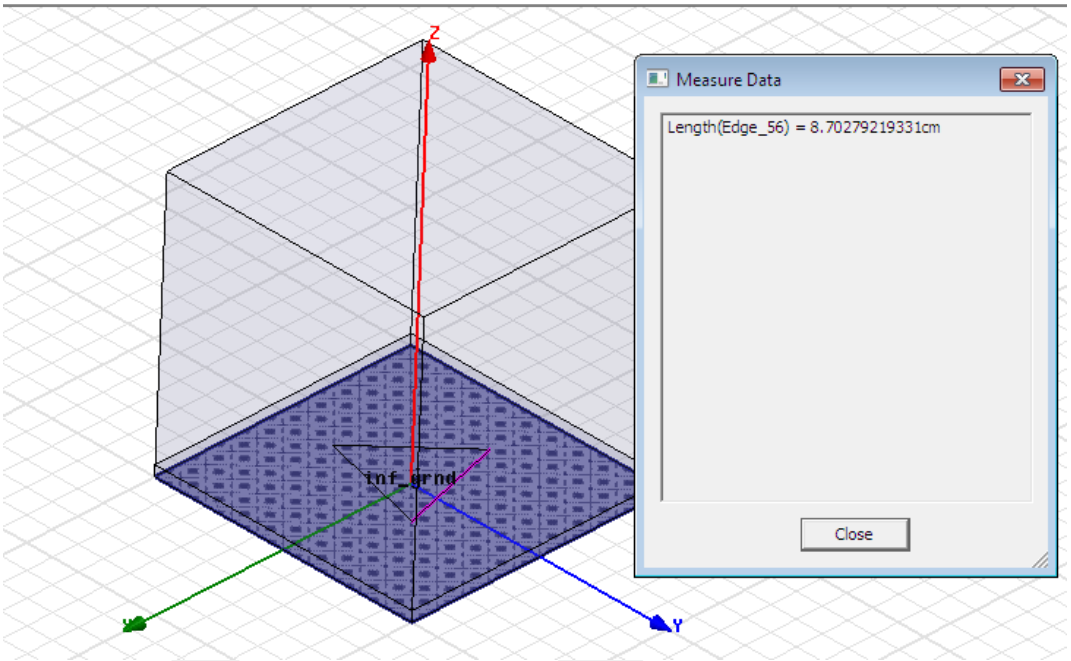

Figure a. 1: Infinitive ground assignment and the side-length of the equilateral triangular patch

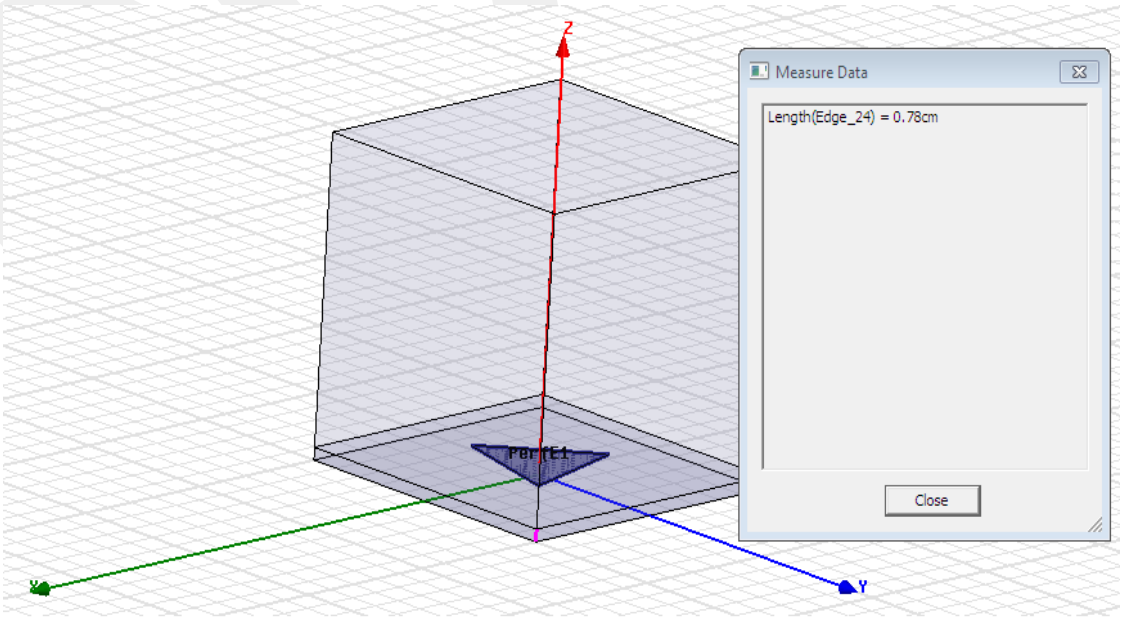

Figure a. 2: Patch assignment (perfect E) and measurement of the thickness of the substrate

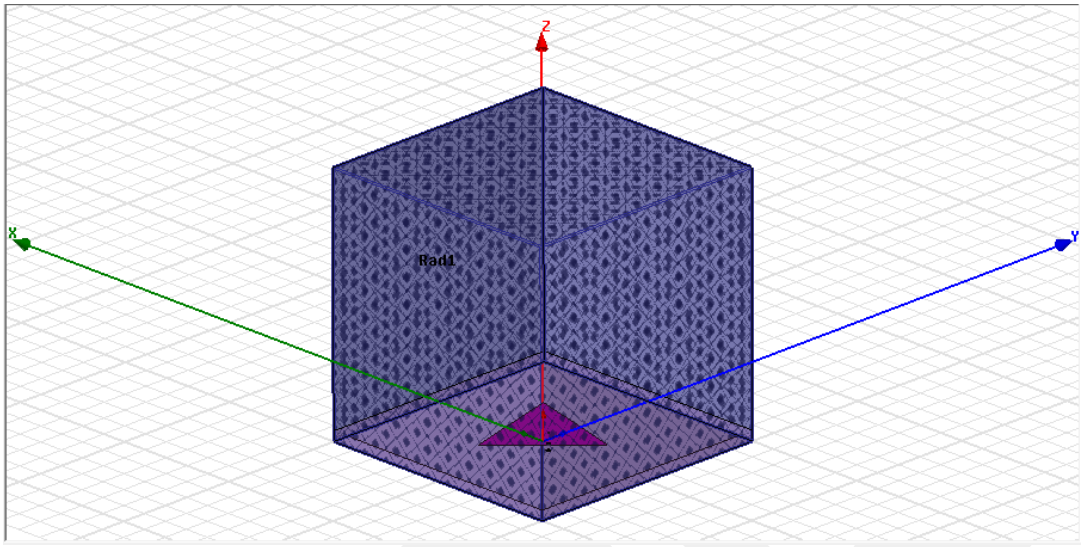

Figure a. 3: Radiation boundary assignment

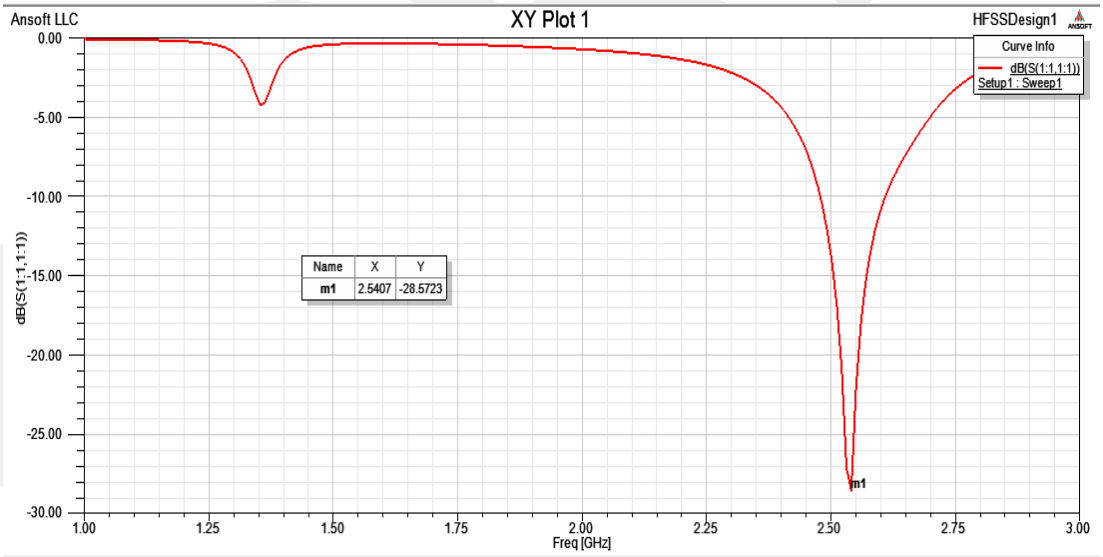

Figure a. 4: Reflection coefficient –frequency graph of the designed antenna